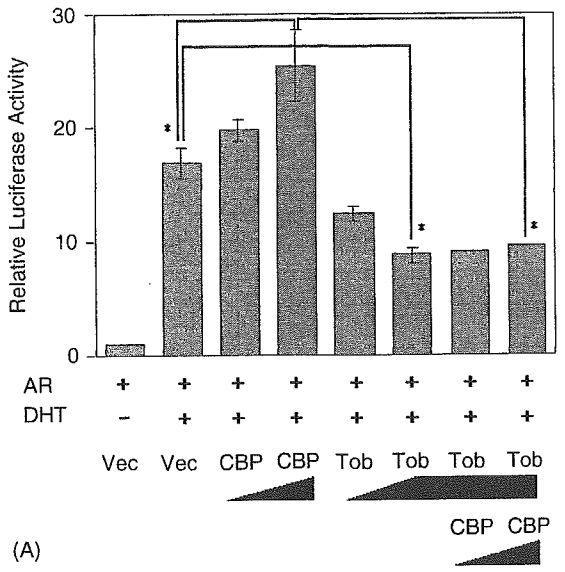

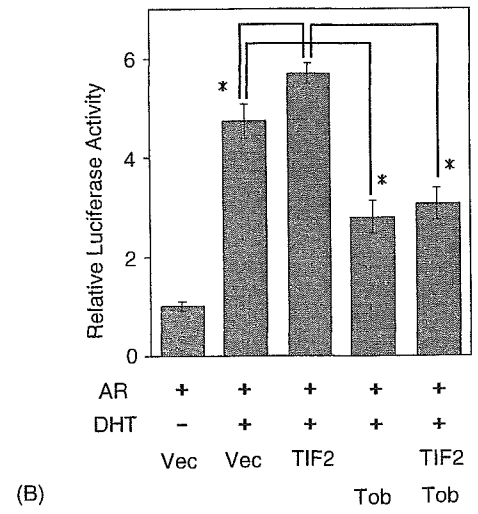

Fig. 5. Effects of coactivator expression on the Tob-mediated repression of the AR-mediated transactivation. (A) pcDNA/mCBP (0.1 or 0.3 μg/well) was cotransfected with pCMV-hAR (0.1 μg/well), pGL3-MMTV and pRL-CMV with or without the Tob expression vector (0.2 or 0.5 μg/well) into MC3T3-E1 cells. The cells were incubated in the absence or presence of DHT for 24 h, and then the luciferase activity was measured. (B) MC3T3-E1 cells were cotransfected with pCMV-hAR (0.1 μg/well), pGL3-MMTV, pRL-CMV, pYFP-Tob1 (0.5 μg/well) and pYFP-TIF2 (0.5 μg/well). After 24 h incubation with DHT, luciferase assay was performed. Bars show the fold change in the luciferase activity relative to the value by the wild type AR without DHT. $^{*}P < 0.05$.

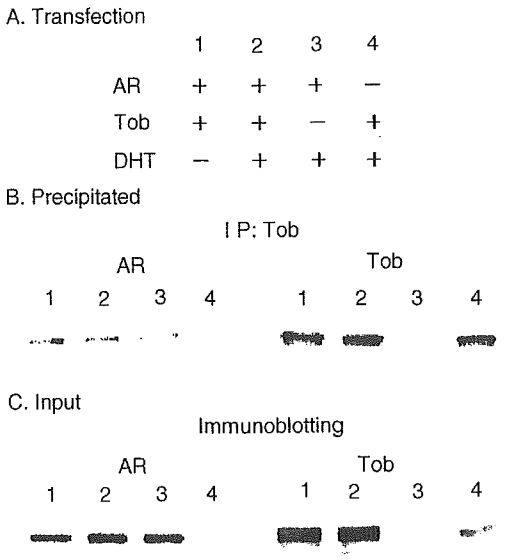

Fig. 6. Coimmunoprecipitation of AR with Tob1 protein. COS-7 cells were transfected with 2 μg of pCMV-hAR and pYFP-Tob1 and then incubated with or without 10^{-8} M DHT for 24 h. The whole cell extracts were subjected to an immunoprecipitation using anti-Tob antibody. Immunoprecipitated fractions were analyzed by immunoblotting as described in Section 2. (A) Transfected (+) and non-transfected (−) expression plasmids, and the presence (+) or absence (−) of ligand in each incubation (lanes 1, 2, 3 or 4) are indicated. (B) AR and Tob in the precipitated fractions were detected by immunoblotting. (C) Input levels of AR and Tob expressed by the transfection (before precipitation) were evaluated by immunoblotting.

regulate the ERα-mediated transcription through the interaction with CAF1, whose yeast homologue is a component of the CCR4-NOT transcription complex. The mutations of LXXLL motifs in BTG1 abolished both the effect of BTG1 on ERα-mediated transactivation and the interaction of BTG1 with CAF1 (Prevot et al., 2001). Tob1 and Tob2 proteins have also been shown to be associated with the CAF1 protein (Ikematsu et al., 1999), therefore, there is a possibility that the modulation of sex steroid hormone receptor-dependent transcription by Tob proteins would be also mediated by the CAF1 protein through an LXXLL motif. However, introduction of mutations into an LXXLL motif of the Tob protein failed to abolish the transcriptional repression. Furthermore PC3/BTG2, which carries two LXXLL motifs, failed to repress AR-mediated transcriptional activation in osteoblastic cells. In the amino acid sequence of the Tob1 protein, we also identified an LXXII motif, which was found in nuclear receptor binding domains of corepressors (Hu and Lazar, 1999; Privalsky, 2004). This LXXII motif was also mutated but repression by the mutant Tob was almost equal to that by the wild type protein. These results indicate that, in osteoblastic cells, the LXXLL and LXXII motifs in the Tob protein are not essential for suppression of nuclear receptor-mediated transactivation, nevertheless, the Tob-induced repression of the

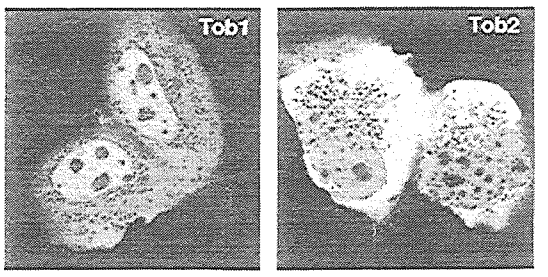

Fig. 7. Localization of wild type Tob1 and Tob2 proteins. YFP-Tob1 or YFP-Tob2 was expressed in MC3T3-C1 osteoblastic cells. Twenty-four hours after the transfection, fluorescent signals in the cells were observed by confocal laser scanning microscopy.

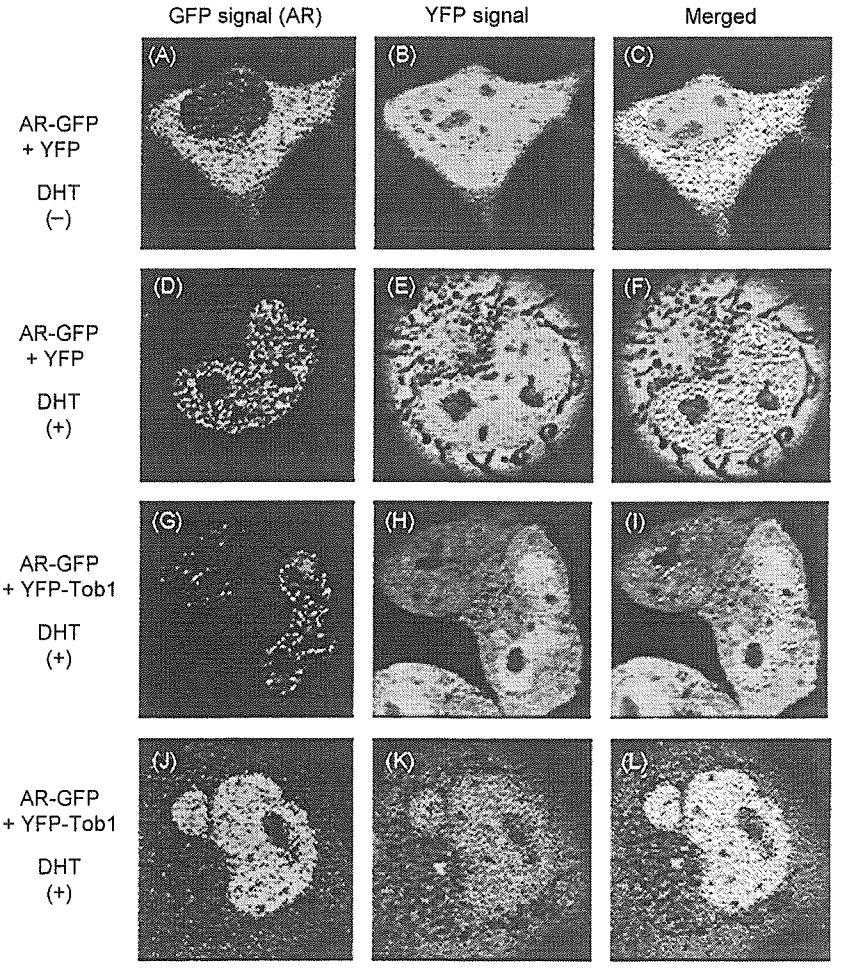

Fig. 8. Subnuclear foci formation of ligand-bound AR and inhibition of the foci formation by expression of the Tob1 protein. The YFP vector (YFP), carrying only a YFP cDNA, and pAR-GFP (AR-GFP) were cotransfected into MC3T3-E1 cells (A–F). Before adding DHT, fluorescent signals from AR-GFP (A) and YFP (B) were collected and the two signals were merged (C). Signals from AR-GFP (D) and YFP (E) in the DHT-treated cells were also collected and the two images were merged (F). MC3T3-E1 cells were cotransfected with pAR-GFP and pYFP-Tob1 (G–L). Fluorescent signals from AR-GFP (G and J) and YFP-Tob1 (H and K) were collected in the presence of DHT, and the two signals were merged (I–L). The experimental conditions were identical between G–I and J–K.

transactivation function of AR was suggested to be mediated by the direct interaction between Tob and AR as demonstrated in the present study by coimmunoprecipitation.

As we previously reported, ligand-dependent intranuclear foci formation of AR closely depends on the receptor being in a transcriptionally active conformation (Tomura et al., 2001; Saitoh et al., 2002). CBP, one of the coactivators for AR, is colocalized with AR at subnuclear foci after treatment with the ligand, and CBP is considered to be essential for the formation of nuclear foci of AR (Saitoh et al., 2002). It was shown that activation of AP-1 or NF-κB repressed AR-mediated transactivation. Extraction of endogenous CBP from the AR-mediated transactivation complex by these transcriptional factors is thought to be a cause of the repression because this repression is relieved by supplementation with exogenous CBP (Frønsdal et al., 1998; Aarnisalo et al., 1998). The dominant negative form of CBP also suppressed AR-mediated transactivation and destroyed AR subnuclear foci, however, cotransfection of a wild type CBP expression vector rescued AR foci formation (Saitoh et al., 2002). In the present paper, we demonstrated that expression of Tob protein inhibited the subnuclear foci formation of AR, being consistent with the results of the luciferase reporter assay. To examine whether CBP is involved in the Tob-induced repression of the transactivation function of AR, CBP was coexpressed with AR and Tob in osteoblastic cells. However, the CBP expression had no effect on the Tob-mediated repression (Fig. 5A). Similarly, the Tob-induced repression of transactivation was not recovered by supplementation of another common coactivator, TIF2 (Fig. 5B). CBP also failed to recover the AR foci formation destroyed by the expression of Tob (data not shown). According to these results, Tob-mediated repression of the AR transactivation function is not due to the sequestration of coactivators from AR transactivation complex. In the present experiments, Tob inhibited the subnuclear foci formation of AR. According to the previous studies including ours, these subnuclear foci are now considered to be the sites where nuclear receptors interact with

coactivators to form (pre)transactivation complexes before binding to DNA (Stenoien et al., 2000; Saitoh et al., 2002). Therefore, Tob seems to inhibit formation of the transcriptionally active complex of AR that should be an earlier step than AR-DNA binding. However, further study will be necessary to elucidate the precise mechanism of the Tob-induced repression of AR-mediated transactivation.

Tob1 knockout mice showed increased bone volume resulting from an increased number of osteoblasts, not due to reduced activity of osteoclasts (Yoshida et al., 2000). Sex steroid hormones are known to promote osteoblast proliferation and differentiation (Hofbauer and Khosla, 1999; Manolagas et al., 2002). Based on our findings that Tob protein represses AR and ERα-dependent transactivation in osteoblastic cells, Tob deficiency would result in upregulation of the transactivation functions of AR and ERα in bone formation. Such elevated function of steroid hormone receptors may also partially contribute to the enhancement of bone volume in Tob-deficient mice.

In conclusion, for the first time, to our knowledge, the present study revealed the repression effects of Tob proteins on sex steroid hormone receptor-mediated transactivation function, thus, Tob proteins would be one of the intracellular modulators for extracellular signals such as BMP-2 and sex steroids.

Acknowledgements

This work was supported in part by grants-in-aid for Scientific Research (B) and Exploratory Research and a grant for the 21st Century Center of Excellence (COE) Program (Kyushu University) from the Japanese Ministry of Education, Culture, Sports, Science and Technology.

References

Aarnisalo, P., Palvimo, J.J., Jänne, O.A., 1998. CREB-binding protein in androgen receptor-mediated signaling. Proc. Natl. Acad. Sci. U.S.A. 95, 2122–2127.

Adachi, M., Takayanagi, R., Tomura, A., Imasaki, K., Kato, S., Goto, K., Yanase, T., Ikuyama, S., Nawata, H., 2000. Androgen-insensitivity syndrome as a possible coactivator disease. N. Engl. J. Med. 343, 856–862.

Aranda, A., Pascual, A., 2001. Nuclear hormone receptors and gene expression. Physiol. Rev. 81, 1269–1304.

Cheng, S., Brzostek, S., Lee, S.R., Hollenberg, A.N., Balk, S.P., 2002. Inhibition of the dihydrotestosterone-activated androgen receptor by nuclear receptor corepressor. Mol. Endocrinol. 16, 1492–1501.

Frønsdal, K., Engedal, N., Slagsvold, T., Saatcioglu, F., 1998. CREB binding protein is a coactivator for the androgen receptor and mediates cross-talk with AP-1. J. Biol. Chem. 273, 31853–31859.

Heinlein, C.A., Chang, C., 2002. Androgen receptor (AR) coregulators: an overview. Endocr. Rev. 23, 175–200.

Hofbauer, L.C., Khosla, S., 1999. Androgen effects on bone metabolism: recent progress and controversies. Eur. J. Endocrinol. 140, 271–286.

Hu, X., Lazar, M.A., 1999. The CoRNR motif controls the recruitment of corepressors by nuclear hormone receptors. Nature 402, 93–96.

Ikematsu, N., Yoshida, Y., Kawamura-Tsuzuku, J., Ohsugi, M., Onda, M., Hirai, M., Fujimoto, J., Yamamoto, T., 1999. Tob2, a novel anti-proliferative Tob/BTG1 family member, associates with a component of the CCR4 transcriptional regulatory complex capable of binding cyclin-dependent kinases. Oncogene 18, 7432–7441.

Kamei, Y., Xu, L., Heinzel, T., Torchia, J., Kurokawa, R., Gloss, B., Lin, S.C., Heyman, R.A., Rose, D.W., Glass, C.K., Rosenfeld, M.G., 1996. A CBP integrator complex mediates transcriptional activation and AP-1 inhibition by nuclear receptors. Cell 85, 403–414.

Kawano, H., Sato, T., Yamada, T., Matsumoto, T., Sekine, K., Watanabe, T., Nakamura, T., Fukuda, T., Yoshimura, K., Yoshizawa, T., Aihara, K.I., Yamamoto, Y., Nakamichi, Y., Metzger, D., Chambon, P., Nakamura, K., Kawaguchi, H., Kato, S., 2003. Suppressive function of androgen receptor in bone resorption. Proc. Natl. Acad. Sci. U.S.A. 100, 9416–9421.

Leo, C., Chen, J.D., 2000. The SRC family of nuclear receptor coactivators. Gene 245, 1–11.

Maekawa, M., Nishida, E., Tanoue, T., 2002. Identification of the anti-proliferative protein Tob as a MAPK substrate. J. Biol. Chem. 277, 37783–37787.

Manolagas, S.C., Kousteni, S., Jilka, R.L., 2002. Sex steroids and bone. Recent Prog. Horm. Res. 57, 385–409.

Matsuda, S., Kawamura-Tsuzuku, J., Ohsugi, M., Yoshida, M., Emi, M., Nakamura, Y., Onda, M., Yoshida, Y., Nishiyama, A., Yamamoto, T., 1996. Tob, a novel protein that interacts with p185erbB2, is associated with anti-proliferative activity. Oncogene 12, 705–713.

Matsuda, S., Rouault, J., Magaud, J., Berthet, C., 2001. In search of a function for the TIS21/PC3/BTG1/Tob family. FEBS Lett. 497, 67–72.

Miyagishi, M., Fujii, R., Hatta, M., Yoshida, E., Araya, N., Nagafuchi, A., Ishihara, S., Nakajima, T., Fukamizu, A., 2000. Regulation of Lef-mediated transcription and p53-dependent pathway by associating beta-catenin with CBP/p300. J. Biol. Chem. 275, 35170–35175.

Nakao, R., Haji, M., Yanase, T., Ogo, A., Takayanagi, R., Katsube, T., Fukumaki, Y., Nawata, H., 1992. A single amino acid substitution (Met786—Val) in the steroid-binding domain of human androgen receptor leads to complete androgen insensitivity syndrome. J. Clin. Endocrinol. Metab. 74, 1152–1157.

Ohnaka, K., Shimoda, S., Nawata, H., Shimokawa, H., Kaibuchi, K., Iwamoto, Y., Takayanagi, R., 2001. Pitavastatin enhanced BMP-2 and osteocalcin expression by inhibition of Rho-associated kinase in human osteoblasts. Biochem. Biophys. Res. Commun. 287, 337–342.

Onoe, Y., Miyaura, C., Ito, M., Ohta, H., Nozawa, S., Suda, T., 2000. Comparative effects of estrogen and raloxifene on B lymphopoiesis and bone loss induced by sex steroid deficiency in mice. J. Bone Miner. Res. 15, 541–549.

Prevot, D., Morel, A.P., Voeltzel, T., Rostan, M.C., Rimokh, R., Magaud, J.P., Corbo, L., 2001. Relationships of the anti-proliferative proteins BTG1 and BTG2 with CAF1, the human homolog of a component of the yeast CCR4 transcriptional complex: involvement in estrogen receptor alpha signaling pathway. J. Biol, Chem. 276, 9640–9648.

Privalsky, M.L., 2004. The role of corepressors in transcriptional regulation by nuclear hormone receptors. Annu. Rev. Physiol. 66, 315–360.

Rouault, J.P., Prevot, D., Berthet, C., Birot, A.M., Billaud, M., Magaud, J.P., Corbo, L., 1998. Interaction of BTG1 and p53-regulated BTG2 gene products with mCaf1, the murine homolog of a component of the yeast CCR4 transcriptional regulatory complex. J. Biol. Chem. 273, 22563–22569.

Saitoh, M., Takayanagi, R., Goto, K., Fukamizu, A., Tomura, A., Yanase, T., Nawata, H., 2002. The presence of both the amino- and carboxyl-terminal domains in the AR is essential for the completion of a transcriptionally active form with coactivators and intranuclear compartmentalization common to the steroid hormone receptors: a three-dimensional imaging study. Mol. Endocrinol. 16, 694–706.

Stenoien, D.L., Mancini, M.G., Patel, K., Allegretto, E.A., Smith, C.L., Mancini, M.A., 2000. Subnuclear trafficking of estrogen receptor-alpha and steroid receptor coactivator-1. Mol. Endocrinol. 14, 518–534.

Suzuki, T., Kawamura-Tsuzuku, J., Ajima, R., Nakamura, T., Yoshida, Y., Yamamoto, T., 2002. Phosphorylation of three regulatory serines of Tob by Erk1 and Erk2 is required for Ras-mediated cell proliferation and transformation. Genes Dev. 16, 1356–1370.

Tirone, F., 2001. The gene PC3 (TIS21/BTG2), prototype member of the PC3/BTG/Tob family: regulator in control of cell growth, differentiation, and DNA repair? J. Cell. Physiol. 187, 155–165.

Tomura, A., Goto, K., Morinaga, H., Nomura, M., Okabe, T., Yanase, T., Takayanagi, R., Nawata, H., 2001. The subnuclear three-dimensional image analysis of androgen receptor fused to green fluorescence protein. J. Biol. Chem. 276, 28395–28401.

Yeh, S., Tsai, M.Y., Xu, Q., Mu, X.M., Lardy, H., Huang, K.E., Lin, H., Yeh, S.D., Altuwaijri, S., Zhou, X., Xing, L., Boyce, B.F., Hung, M.C., Zhang, S., Gan, L., Chang, C., Hung, M.C., 2002. Generation and characterization of androgen receptor knockout (ARKO) mice: an in vivo model for the study of androgen functions in selective tissues. Proc. Natl. Acad. Sci. U.S.A. 99, 13498–13503.

Yoshida, Y., Tanaka, S., Umemori, H., Minowa, O., Usui, M., Ikematsu, N., Hosoda, E., Imamura, T., Kuno, J., Yamashita, T., Miyazono, K., Noda, M., Noda, T., Yamamoto, T., 2000. Negative regulation of BMP/Smad signaling by Tob in osteoblasts. Cell 103, 1085–1097.

Yoshida, Y., Nakamura, T., Komoda, M., Satoh, H., Suzuki, T., Tsuzuku, J.K., Miyasaka, T., Yoshida, E.H., Umemori, H., Kunisaki, R.K., Tani, K., Ishii, S., Mori, S., Suganuma, M., Noda, T., Yamamoto, T., 2003. Mice lacking a transcriptional corepressor Tob are predisposed to cancer. Genes Dev. 17, 1201–1206.

Available online at www.sciencedirect.com
SCIENCE DIRECT®
Biochemical and Biophysical Research Communications 329 (2005) 177–181
BBRC
www.elsevier.com/locate/ybbrc

Glucocorticoid suppresses the canonical Wnt signal in cultured human osteoblasts

Keizo Ohnaka[a,*], Mizuho Tanabe[a], Hisaya Kawate[a], Hajime Nawata[b], Ryoichi Takayanagi[a]

[a] *Department of Geriatric Medicine, Graduate School of Medical Sciences, Kyushu University, 3-1-1 Maidashi, Higashi-ku, Fukuoka 812-8582, Japan*
[b] *Department of Medicine and Bioregulatory Science, Graduate School of Medical Sciences, Kyushu University, 3-1-1 Maidashi, Higashi-ku, Fukuoka 812-8582, Japan*

Received 22 January 2005

Abstract

To explore the mechanism of glucocorticoid-induced osteoporosis, we investigated the effect of glucocorticoid on canonical Wnt signaling that emerged as a novel key pathway for promoting bone formation. Wnt3a increased the T-cell factor (Tcf)/lymphoid enhancer factor (Lef)-dependent transcriptional activity in primary cultured human osteoblasts. Dexamethasone suppressed this transcriptional activity in a dose-dependent manner, while 1,25-dihydroxyvitamin D3 increased this transcriptional activity. LiCl, an inhibitor of glycogen synthase kinase-3β, also enhanced the Tcf/Lef-dependent transcriptional activity, which was, however, not inhibited by dexamethasone. The addition of anti-dickkopf-1 antibody partially restored the transcriptional activity suppressed by dexamethasone. Dexamethasone decreased the cytosolic amount of β-catenin accumulated by Wnt3a and also inhibited the nuclear translocation of β-catenin induced by Wnt3a. These data suggest that glucocorticoid suppresses the canonical Wnt signal in cultured human osteoblasts, partially through the enhancement of the dickkopf-1 production.

Keywords: Glucocorticoid; Wnt; Dickkopf-1; Osteoblast; Osteoporosis

Osteoporosis is one of the most frequent and serious side effects of long-term glucocorticoid therapy [1]. Glucocorticoids have profound effects on bone metabolism [2]. Glucocorticoid excess increases bone resorption and decreases bone formation; consequently rapid bone loss occurs. Nowadays, a direct inhibition of osteoblast activity by glucocorticoids is the most favored principal mechanism of glucocorticoid-induced osteoporosis [1–3]. However, detailed mechanism by which they inhibit osteoblast function remains to be fully elucidated.

Recent progress uncovers the importance of Wnt signaling in skeletal biology [4,5]. The loss-of-function mutations in human LDL receptor-related protein 5 (LRP5) gene cause osteoporosis-pseudoglioma syndrome (OPPG) characterized by low bone mass and abnormal eye development, while the gain-of-function mutations in this gene give rise to high bone mass syndrome [6–8]. Furthermore, the LRP5 gene knockout mice show the phenotype of low bone mass resembling that of human OPPG [9]. These findings highlighted Wnt signaling as another key pathway involved in the regulation of postnatal bone mass.

The Wnt signal transduction comprises three intracellular pathways: the canonical pathway, the Wnt/planar-cell-polarity (PCP) pathway, and the Wnt/Ca^{2+} pathway [10,11]. Although which pathway is involved in bone formation remains to be fully elucidated, recent studies strongly suggest that the canonical pathway plays a central role in promoting bone formation [4,5,12]. Canonical Wnts bind to frizzled/LRP5 receptor complex, inactivate glycogen synthase kinase-3β

* Corresponding author. Fax: +81 92 642 6911.
E-mail address: oonaka@geriat.med.kyushu-u.ac.jp (K. Ohnaka).

0006-291X/$ - see front matter © 2005 Elsevier Inc. All rights reserved.
doi:10.1016/j.bbrc.2005.01.117

(GSK-3β), and inhibit phosphorylation and consequential degradation of intracellular β-catenin [10,11]. Accumulated β-catenin translocates into the nucleus and activates target genes by a complex formed with transcription factors of the T-cell factor (Tcf)/lymphoid enhancer factor (Lef) family [10,11].

Wnt signals are extracellularly regulated by several secreted antagonists including secreted frizzled-related protein (sFRP), Cerberus, Wnt inhibitory factor-1 (WIF-1), and dickkopf (Dkk) [13]. We have reported that glucocorticoid enhances the expression of dickkopf-1 (Dkk-1) in cultured human osteoblasts [14]. We extended our exploration of the effect of glucocorticoid on Wnt signaling, and found that glucocorticoid suppresses the canonical Wnt signal, in part mediated by the enhancement of the Dkk-1 production, in cultured human osteoblasts.

Materials and methods

Materials. Eagle's α-MEM, penicillin, and streptomycin were obtained from Invitrogen (Carlsbad, CA). Fetal calf serum (FCS) was purchased from Sanko Junyaku (Tokyo, Japan). Dexamethasone, 17β-estradiol, dihydrotestosterone, 1,25-dihydroxyvitamin D3, LiCl, and goat immunoglobulin (IgG) were purchased from Sigma (St. Louis, MI). Anti-β-catenin monoclonal antibody and anti-Dkk-1 goat polyclonal antibody were purchased from Transduction Laboratories (Lexington, KY) and Santa Cruz Biotechnology (Santa Cruz, CA), respectively. All other reagents were of analytical grade.

Cell culture. Human osteoblasts were prepared from the bone fragments of femur neck as described previously [15]. The cells were grown in Eagle's α-MEM with 10% FCS, 100 mU/ml penicillin, and 100 mU/ml streptomycin. The Wnt3a-expressing cell line (L Wnt-3A cell) and the control cell line (L cell) were obtained from American Type Culture Collection (Manassas, VA). Wnt3a-conditioned medium (Wnt3a-CM) and the control-conditioned medium (C-CM) were harvested according to the manufacturer's instructions. Wnt3a-CM was used in experiments at 10% final concentration, which gave the maximal effect on the Tcf/Lef-dependent transcriptional activity in preliminary studies (data not shown).

Plasmid constructs. The entire coding region of human β-catenin was amplified by reverse transcriptase-polymerase chain reaction (RT-PCR) using KOD-plus DNA polymerase (Toyobo, Tokyo, Japan), confirmed by DNA sequencing, and subcloned into *Sca*I/*Bam*HI sites of pEGFP-C3 (Clontech, Palo Alto, CA) expression vector (designated as pEGFP-β-catenin). TOPflash, a Tcf-binding site reporter plasmid, was purchased from Upstate Biotechnology (Lake Placid, NY).

Transient transfection and reporter assay. Human osteoblasts were transiently transfected by means of calcium phosphate precipitation as described previously [14]. Reporter assay was performed by a dual luciferase assay kit (Promega, MI) according to the manufacturer's instructions.

Subcellular fractionation and immunoblot analysis. Subcellular fractionation and immunoblot analysis were performed essentially as described previously [15]. Soluble (cytosolic) proteins were subjected to sodium dodecyl sulfate–polyacrylamide gel electrophoresis (SDS–PAGE) and proteins in the gel were transferred to a Hybond ECL nitrocellulose membrane (Amersham Biosciences Corp., Piscataway, NJ) through electroblotting. For detection of β-catenin, blots were probed with an anti-β-catenin monoclonal antibody at a dilution of 1:1000. The protein concentration was determined by a BCA protein assay kit (Pierce, Rockford, IL).

Confocal laser microscopic imaging. Human osteoblasts were cultured in 35-mm glass-bottomed dishes (Asahi Techno Glass, Tokyo, Japan) and transfected with pEGFP-β-catenin plasmid vector. The cells were maintained in α-MEM supplemented with 10% charcoal-treated FCS for 24 h and observed with a confocal laser scanning microscope (LSM 510 META, Carl Zeiss, Jena, Germany) as described previously [16].

Statistical analysis. Data are expressed as means ± SD. Statistical analyses were performed with ANOVA followed by Fisher's protected least significant difference test. Significance was accepted at $P < 0.05$.

Results

To investigate the effect of glucocorticoid on canonical Wnt signaling, we first examined whether glucocorticoid would affect the Tcf/Lef-dependent transcriptional activity by a Tcf-reporter gene (luciferase) assay in cultured osteoblasts (Fig. 1A). In primary cultured human osteoblasts, the addition of Wnt3a-conditioned medium (Wnt3a-CM) enhanced the Tcf/Lef-dependent transcriptional activity (approximately 3.5-fold). Dexamethasone suppressed the Wnt3a-induced Tcf/Lef-dependent transcriptional activity in a dose-dependent manner, and dexamethasone at 10^{-7} M suppressed the Wnt3a-stimulated transcriptional activity to the unstimulated basal level.

We also examined the effect of other steroid hormones on the Tcf/Lef-dependent transcriptional activity (Fig. 1B). The addition of 17β-estradiol or dihydrotestosterone did not affect the transcriptional activity stimulated by Wnt3a. The addition of 1,25-dihydroxyvitamin D3 (10^{-7} M) enhanced the Wnt3a-induced reporter activity in cultured human osteoblasts. Furthermore, 1,25-dihydroxyvitamin D3 partially restored the suppressed Wnt3a-induced transcriptional activity by dexamethasone.

Wnt proteins enhance Tcf/Lef-dependent transcription by the canonical signal cascade, namely, the inhibition of GSK-3β, its consequential accumulation of cytosolic β-catenin, translocation of the accumulated β-catenin into the nucleus, and its activation of Tcf/Lef. Therefore, we examined whether or not dexamethasone would affect the intracellular β-catenin level in cultured human osteoblasts. As shown in Fig. 2, the addition of Wnt3a-CM increased the amount of cytosolic β-catenin protein in human osteoblasts. Co-treatment with dexamethasone (10^{-9}–10^{-7} M) dose-dependently decreased the cytosolic level of β-catenin and dexamethasone at 10^{-7} M almost completely reduced to the unstimulated basal level, which is parallel to the suppressive effect of dexamethasone on the reporter luciferase activity. When pEGFP-β-catenin was transfected into human osteoblasts, the GFP-β-catenin was localized most abundantly in the cytosol (Fig. 3). The addition of Wnt3a-CM translocated the GFP-β-catenin into the nucleus, however, co-treatment with

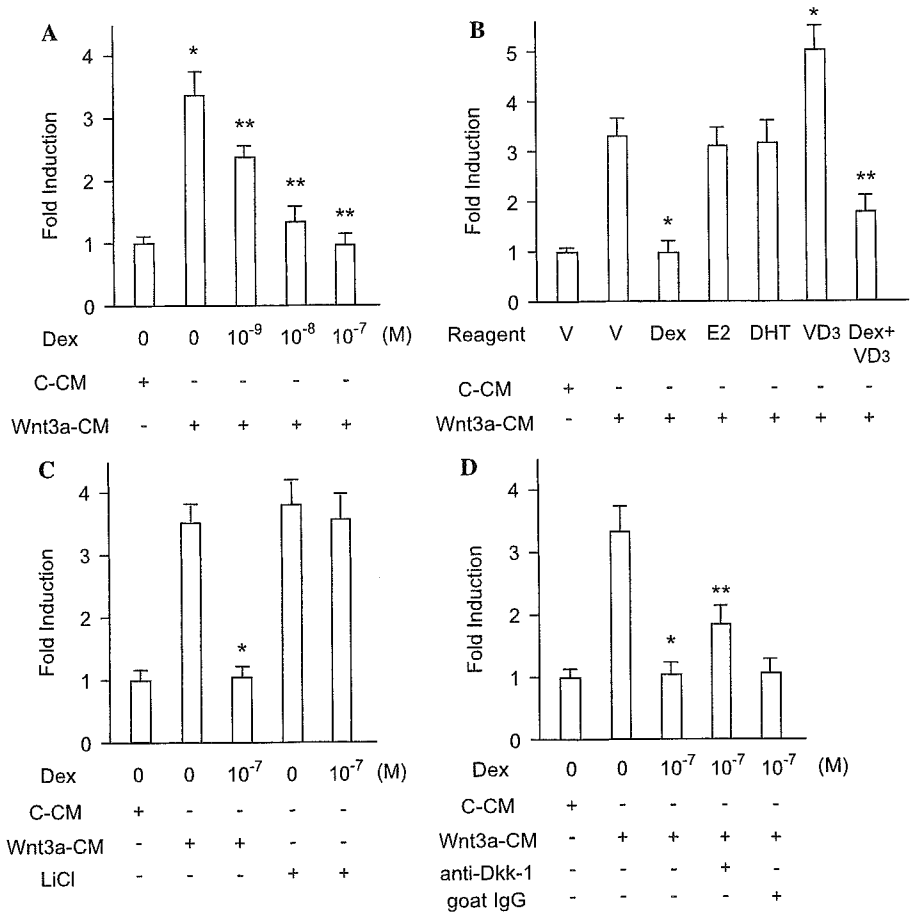

Fig. 1. Effects of Wnt3a, steroid hormones, LiCl, and anti-Dkk-1 antibody on the Tcf/Lef-dependent transcriptional activity in primary cultured human osteoblasts. Human osteoblasts were transfected with TOPflash plasmid vector, and incubated for 36 h with the control-conditioned medium (C-CM) or Wnt3a-conditioned medium (Wnt3a-CM) in the presence of vehicle (ethanol) or various reagents indicated. The reporter luciferase activity was expressed as fold over the activity of TOPflash with C-CM and vehicle. Data are expressed as means ± SD ($n = 4$). One representative data of three independent experiments are shown. (A) 10^{-9}–10^{-7} M dexamethasone (Dex). *$P < 0.01$ vs. C-CM with vehicle. **$P < 0.01$ vs. Wnt3a-CM with vehicle. (B) Vehicle (V, ethanol), 10^{-7} M dexamethasone (Dex), 10^{-7} M 17β-estradiol (E2), 10^{-7} M dihydrotestosterone (DHT), or 10^{-7} M 1,25-dihydroxyvitamin D3 (VD3). *$P < 0.01$ vs. Wnt3a-CM with vehicle. **$P < 0.05$ vs. Wnt3a-CM with Dex. (C) Twenty-five millimolar of LiCl in the presence of vehicle (ethanol) or 10^{-7} M dexamethasone (Dex). *$P < 0.01$ vs. Wnt3a-CM with vehicle. (D) 10^{-7} M dexamethasone (Dex) in combination with anti-Dkk-1 goat polyclonal antibody (anti-Dkk-1) or non-immune goat IgG (goat IgG). *$P < 0.01$ vs. Wnt3a-CM with vehicle. **$P < 0.05$ vs. Wnt3a-CM with Dex.

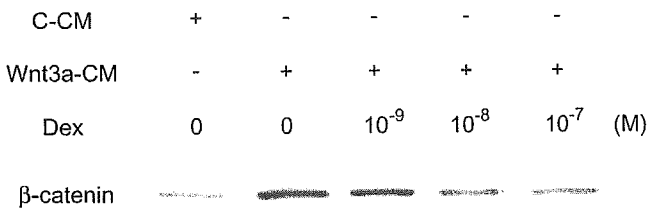

Fig. 2. Effect of dexamethasone on the level of the cytosolic β-catenin protein in primary cultured human osteoblasts. Human osteoblasts were incubated with the control-conditioned medium (control-CM) or Wnt3a-conditioned medium (Wnt3a-CM) in the presence of vehicle (ethanol) or 10^{-9}–10^{-7} M dexamethasone (Dex) for 24 h, and fractionated to soluble and particulate fractions. Soluble proteins (20 μg) were loaded in each lane and subjected to SDS–PAGE (7.5% separating gel). Immunoblot analyses were performed using a specific anti-β-catenin monoclonal antibody. Results shown are representative of three independent experiments.

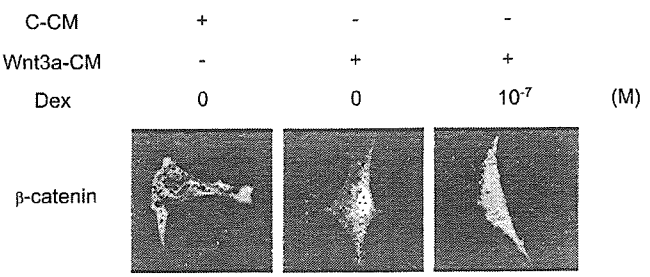

Fig. 3. Effect of dexamethasone on the localization of β-catenin in primary cultured human osteoblasts. Human osteoblasts were transfected with the pEGFP-β-catenin expression vector, and incubated for 24 h with the control-conditioned medium (control-CM) or Wnt3a-conditioned medium (Wnt3a-CM) in the presence of vehicle (ethanol) or 10^{-7} M dexamethasone (Dex). The cells were analyzed by laser confocal microscopy. A representative imaging of three independent experiments is shown (magnification, 100×).

dexamethasone at 10^{-7} M completely inhibited the nuclear translocation of cytosolic β-catenin (Fig. 3). These data suggest that dexamethasone suppressed the Tcf/Lef-dependent transcription through the canonical Wnt signaling cascade rather than by affecting via other signaling pathway(s) or inhibiting directly the Tcf/Lef expression in human osteoblasts.

To further assess the effect of dexamethasone on canonical Wnt signaling, we observed the effect of dexamethasone on the Tcf reporter activity in the presence of LiCl, an inhibitor of GSK-3β, in human osteoblasts (Fig. 1C). The addition of 25 mM LiCl increased the Tcf/Lef-dependent transcriptional activity comparable to that by Wnt3a-CM. However, this increase by LiCl was not suppressed by the treatment with dexamethasone at 10^{-7} M. Since glucocorticoid enhances the expression of Dkk-1, an antagonist of Wnt signaling in human osteoblast [14], we examined the involvement of Dkk-1 in suppressive effect of dexamethasone on canonical Wnt signaling. The addition of anti-Dkk-1-specific goat polyclonal antibody in part (35–45%) restored the suppression of Wnt3a-induced Tcf/Lef-dependent transcriptional activity by dexamethasone, while non-specific goat IgG had no effect on it (Fig. 1D).

Discussion

In the present study, we demonstrated that dexamethasone suppressed the Tcf/Lef-dependent canonical Wnt signaling pathway in primary cultured human osteoblasts. This effect was in part attributed to the increase of Dkk-1 expression by dexamethasone.

Glucocorticoid suppresses osteoblastic differentiation and proliferation by affecting multiple aspects of osteoblast function [1–3]. One well-known effect of glucocorticoid on osteoblast is the inhibition of the expression for Runx2/Cbfa1 [17], a crucial transcriptional factor for differentiation of osteoblast lineage [18]. Runx2/Cbfa1 promotes early osteoblast differentiation from undifferentiated mesenchymal cells, but rather inhibits late osteoblast maturation [18,19]. On the other hand, the Wnt signal plays an essential role in postnatal bone accrual in a Runx2/Cbfa1-independent manner [9]. Our data suggest that glucocorticoid at a therapeutic pharmacological dose may almost completely suppress the canonical Wnt signaling pathway promoting postnatal bone formation in human osteoblasts.

Dexamethasone did not affect the enhancement of Tcf/Lef-dependent transcriptional activity by LiCl, a GSK-3β inhibitor. Therefore, it is presumed that the dexamethasone affects canonical Wnt signaling through GSK-3β itself or upstream of GSK-3β. Indeed, it was reported that glucocorticoid activates GSK-3β and inhibits cell cycle progression in murine preosteoblastic MC3T3-E1 cells [20]. We have previously shown that glucocorticoid enhances the expression of Dkk-1, a secreted antagonist of Wnt signaling, in cultured human osteoblasts [14]. Treatment with anti-Dkk-1-specific antibody partially (approximately 40%) restored the suppression by dexamethasone of Wnt3a-induced Tcf/Lef-dependent transcriptional activity. Although there are several secreted antagonists of Wnt signaling [13] and we did not examine the involvement of other antagonists than Dkk-1 proteins, our data suggest that the inhibition of the canonical Wnt signal by glucocorticoid may be in part through the antagonistic effect of the enhanced Dkk-1 production in cultured human osteoblasts.

Interestingly, 1,25-dihydroxyvitamin D3 enhanced the Tcf/Lef-dependent transcriptional activity induced by Wnt3a in cultured human osteoblasts. Furthermore, 1,25-dihydroxyvitamin D3 restored the suppressed Wnt3a-induced transcriptional activity by dexamethasone. Previous study reported that the vitamin D receptor with its ligand inhibits β-catenin-Tcf/Lef-dependent gene transcription in colon carcinoma cells [21]. The vitamin D effect on Wnt signaling may be different by the types of cell and target genes, which will require further investigations. Active vitamin D metabolites are used for prevention and treatment of glucocorticoid-induced osteoporosis [22,23]. Besides the known effects of vitamin D3 on bone and mineral metabolism [23], the effect on Wnt signaling may contribute to the clinical effect of vitamin D3 for the treatment of osteoporosis.

LRP5 knockout mice show low bone mass due to decreased osteoblast proliferation [9], but the precise mechanism whereby the Wnt/LRP5 signal promotes bone formation remains to be fully clarified. However, given the significance of the canonical Wnt signaling pathway in postnatal control of bone formation, strong inhibition of this pathway by glucocorticoid may in part explain the impairment of osteoblastic function and bone formation induced by glucocorticoid excess. Our findings in this study and further investigations will provide clues to new strategies for the treatment of glucocorticoid-induced osteoporosis.

Acknowledgments

This work was supported in part by Grants-in-Aid for Scientific Research (B), Scientific Research (C) and Exploratory Research, and a grant for the 21st Century Center of Excellence (COE) Program (Kyushu University) from the Japanese Ministry of Education, Culture, Sports, Science and Technology.

References

[1] K.G. Saag, Glucocorticoid-induced osteoporosis, Endocrinol. Metab. Clin. North Am. 32 (2003) 135–157.

[2] E. Canalis, Clinical review 83: Mechanisms of glucocorticoid action in bone: Implications to glucocorticoid-induced osteoporosis, J. Clin. Endocrinol. Metab. 81 (1996) 3441–3447.
[3] S.C. Manolagas, R.S. Weinstein, New developments in the pathogenesis and treatment of steroid-induced osteoporosis, J. Bone Miner. Res. 14 (1999) 1061–1066.
[4] M.L. Johnson, K. Harnish, R. Nusse, W. Van Hul, LRP5 and Wnt signaling: A union made for bone, J. Bone Miner. Res. 19 (2004) 1749–1757.
[5] J.J. Westendorf, R.A. Kahler, T.M. Schroeder, Wnt signaling in osteoblasts and bone diseases, Gene 341 (2004) 19–39.
[6] Y. Gong, R.B. Slee, N. Fukai, G. Rawadi, S. Roman-Roman, A.M. Reginato, H. Wang, T. Cundy, F.H. Glorieux, D. Lev, M. Zacharin, K. Oexle, J. Marcelino, W. Suwairi, S. Heeger, G. Sabatakos, S. Apte, W.N. Adkins, J. Allgrove, M. Arslan-Kirchner, J.A. Batch, P. Beighton, G.C. Black, R.G. Boles, L.M. Boon, C. Borrone, H.G. Brunner, G.F. Carle, B. Dallapiccola, A. De Paepe, B. Floege, M.L. Halfhide, B. Hall, R.C. Hennekam, T. Hirose, A. Jans, H. Juppner, C.A. Kim, K. Keppler-Noreuil, A. Kohlschuetter, D. LaCombe, M. Lambert, E. Lemyre, T. Letteboer, L. Peltonen, R.S. Ramesar, M. Romanengo, H. Somer, E. Steichen-Gersdorf, B. Steinmann, B. Sullivan, A. Superti-Furga, W. Swoboda, M.J. van den Boogaard, W. Van Hul, M. Vikkula, M. Votruba, B. Zabel, T. Garcia, R. Baron, B.R. Olsen, M.L. Warman, LDL receptor-related protein 5 (LRP5) affects bone accrual and eye development, Cell 107 (2001) 513–523.
[7] L.M. Boyden, J. Mao, J. Belsky, L. Mitzner, A. Farhi, M.A. Mitnick, D. Wu, K. Insogna, R.P. Lifton, High bone density due to a mutation in LDL-receptor-related protein 5, N. Engl. J. Med. 346 (2002) 1513–1521.
[8] R.D. Little, J.P. Carulli, R.G. Del Mastro, J. Dupuis, M. Osborne, C. Folz, S.P. Manning, P.M. Swain, S.C. Zhao, B. Eustace, M.M. Lappe, L. Spitzer, S. Zweier, K. Braunschweiger, Y. Benchekroun, X. Hu, R. Adair, L. Chee, M.G. FitzGerald, C. Tulig, A. Caruso, N. Tzellas, A. Bawa, B. Franklin, S. McGuire, X. Nogues, G. Gong, K.M. Allen, A. Anisowicz, A.J. Morales, P.T. Lomedico, S.M. Recker, P. Van Eerdewegh, R.R. Recker, M.L. Johnson, A mutation in the LDL receptor-related protein 5 gene results in the autosomal dominant high-bone-mass trait, Am. J. Hum. Genet. 70 (2002) 11–19.
[9] M. Kato, M.S. Patel, R. Levasseur, I. Lobov, B.H. Chang, D.A. Glass, C. Hartmann, L. Li, T.H. Hwang, C.F. Brayton, R.A. Lang, G. Karsenty, L. Chan, Cbfa1-independent decrease in osteoblast proliferation, osteopenia, and persistent embryonic eye vascularization in mice deficient in Lrp5, a Wnt coreceptor, J. Cell Biol. 157 (2002) 303–314.
[10] A. Wodarz, R. Nusse, Mechanisms of Wnt signaling in development, Annu. Rev. Cell Dev. Biol. 14 (1998) 59–88.
[11] A. Bejsovec, Wnt signaling: An embarrassment of receptors, Curr. Biol. 10 (2000) R919–R922.
[12] H. Hu, M.J. Hilton, X. Tu, K. Yu, D.M. Ornitz, F. Long, Sequential roles of Hedgehog and Wnt signaling in osteoblast development, Development 132 (2005) 49–60.
[13] Y. Kawano, R. Kypta, Secreted antagonists of the Wnt signalling pathway, J. Cell Sci. 116 (2003) 2627–2634.
[14] K. Ohnaka, H. Taniguchi, H. Kawate, H. Nawata, R. Takayanagi, Glucocorticoid enhances the expression of dickkopf-1 in human osteoblasts: Novel mechanism of glucocorticoid-induced osteoporosis, Biochem. Biophys. Res. Commun. 318 (2004) 259–264.
[15] K. Ohnaka, S. Shimoda, H. Nawata, H. Shimokawa, K. Kaibuchi, Y. Iwamoto, R. Takayanagi, Pitavastatin enhanced BMP-2 and osteocalcin expression by inhibition of Rho-associated kinase in human osteoblasts, Biochem. Biophys. Res. Commun. 287 (2001) 337–342.
[16] H. Kawate, Y. Wu, K. Ohnaka, H. Nawata, R. Takayanagi, Tob proteins suppress steroid hormone receptor-mediated transcriptional activation, Mol. Cell. Endocrinol. 230 (2005) 77–86.
[17] D.J. Chang, C. Ji, K.K. Kim, S. Casinghino, T.L. McCarthy, M. Centrella, Reduction in transforming growth factor β receptor I expression and transcription factor CBFa1 on bone cells by glucocorticoid, J. Biol. Chem. 273 (1998) 4892–4896.
[18] T. Komori, H. Yagi, S. Nomura, A. Yamaguchi, K. Sasaki, K. Deguchi, Y. Shimizu, R.T. Bronson, Y.H. Gao, M. Inada, M. Sato, R. Okamoto, Y. Kitamura, S. Yoshiki, T. Kishimoto, Targeted disruption of Cbfa1 results in a complete lack of bone formation owing to maturational arrest of osteoblasts, Cell 89 (1997) 755–764.
[19] W. Liu, S. Toyosawa, T. Furuichi, N. Kanatani, C. Yoshida, Y. Liu, M. Himeno, S. Narai, A. Yamaguchi, T. Komori, Overexpression of Cbfa1 in osteoblasts inhibits osteoblast maturation and causes osteopenia with multiple fractures, J. Cell Biol. 155 (2001) 157–166.
[20] E. Smith, G.A. Coetzee, B. Frenkel, Glucocorticoids inhibit cell cycle progression in differentiating osteoblasts via glycogen synthase kinase-3 β, J. Biol. Chem. 277 (2002) 18191–18197.
[21] H.G. Palmer, J.M. Gonzalez-Sancho, J. Espada, M.T. Berciano, I. Puig, J. Baulida, M. Quintanilla, A. Cano, A.G. de Herreros, M. Lafarga, A. Munoz, Vitamin D3 promotes the differentiation of colon carcinoma cells by the induction of E-cadherin and the inhibition of β-catenin signaling, J. Cell Biol. 154 (2001) 369–387.
[22] J.Y. Reginster, C. de Froidmont, M.P. Lecart, N. Sarlet, J.O. Defraigne, Alphacalcidol in prevention of glucocorticoid-induced osteoporosis, Calcif. Tissue Int. 65 (1999) 328–331.
[23] R.N. de Nijs, J.W. Jacobs, A. Algra, W.F. Lems, J.W. Bijlsma, Prevention and treatment of glucocorticoid-induced osteoporosis with active vitamin D3 analogues: A review with meta-analysis of randomized controlled trials including organ transplantation studies, Osteoporos. Int. 15 (2004) 589–602.

Available online at www.sciencedirect.com
SCIENCE DIRECT®
ELSEVIER
Biochemical and Biophysical Research Communications 331 (2005) 1025–1031
BBRC
www.elsevier.com/locate/ybbrc

A zinc finger protein TZF is a novel corepressor of androgen receptor

Masamichi Ishizuka [a,1], Hisaya Kawate [b,1], Ryoichi Takayanagi [b], Hirotaka Ohshima [a], Rong-Hua Tao [b], Hiromi Hagiwara [a,c,*]

[a] *Department of Biological Sciences, Tokyo Institute of Technology, 4259 Nagatsuta-cho, Midori-ku, Yokohama 226-8501, Japan*
[b] *Department of Geriatric Medicine, Graduate School of Medical Sciences, Kyushu University, Maidashi 3-1-1, Higashi-ku, Fukuoka 812-8582, Japan*
[c] *Department of Biomedical Engineering, Toin University of Yokohama, 1614 Kurogane-cho, Aoba-ku, Yokohama 225-8502, Japan*

Received 2 April 2005
Available online 13 April 2005

Abstract

Steroid hormones control the transcriptional activity of target genes mediated by intracellular nuclear receptors, and these transcriptional activities are modulated by the combination with coactivators and corepressors. We found in this study that testicular zinc finger protein (TZF) that was a nuclear protein with a zinc finger motif of the Cys_2-His_2 type was a novel corepressor of androgen receptor (AR). Fusion protein with green fluorescence protein GFP formed the specific foci in nuclei and TZF-dependent foci were located close to the splicing factor compartment. In addition, TZF was recruited into AR subnuclear foci after the treatment of dihydrotestosterone. Furthermore, we revealed that TZF bound to the activation function-1 (AF-1) domain (N-terminal transactivating domain) of AR protein. Transient over-expression of TZF in COS-7 cells or LNCaP human prostatic cancer cell resulted in decreased AR activity in a ligand-dependent fashion. Moreover, a transcriptional corepressor N-CoR additively decreased the transcriptional activity of AR with TZF. These findings suggest that TZF might be a novel corepressor of AR.

Keywords: Zinc finger protein; Corepressor; Androgen; Androgen receptor; Transcriptional activity

The actions of steroid hormones are mediated by intracellular nuclear receptors whose coordinate activity defines the physiological response [1]. These receptors are all structurally related and constitute a superfamily of nuclear regulatory proteins that modulate gene expression in a ligand-dependent fashion. In the case of androgen receptor (AR), it has been proposed that ligand binds to the cytosolic AR, and then the receptor–ligand complex is relocated to the nucleus with subsequent sequence-specific interaction with hormone responsive elements of target genes under the control of various cofactors to regulate the transcription of target genes [2,3]. A number of transcriptional cofactors (coactivators and corepressors) have been identified and they include the p160 family [4–6], CBP/p300 [7], PCAF/GCN5 [8], and TRAPs/DRIPs [9] as the coactivator, and SMRT/Sin3A [10,11] and N-CoR [12,13] as the corepressor. These transcriptional cofactors are organized in multiprotein complexes and facilitate the access of nuclear receptors and the RNA polymerase II core machinery to their target DNA sequences by chromatin remodeling and histone modification. Transcriptional repression is an intrinsic part of endocrine physiology. However, the mechanism of repression is not fully understood. One reason is the lack of number of corepressors found.

AR, like other steroid hormone receptors, contains the following structural and functional domains: a central DNA-binding domain, a C-terminal ligand-binding domain, and two potential transcriptional activation domains (AF-1 and AF-2). AF-1 is located in the N-terminal region of the receptor and has been shown to act in a

* Corresponding author. Fax: +81 45 972 5972.
E-mail address: hagiwara@cc.toin.ac.jp (H. Hagiwara).
[1] These authors contributed equally to this work.

0006-291X/$ - see front matter © 2005 Elsevier Inc. All rights reserved.
doi:10.1016/j.bbrc.2005.04.024

ligand-independent fashion. By contrast, a ligand-dependent AF-2 domain, which colocalizes with the highly conserved C-terminal ligand-binding domain, is predicted from the sequence similarity among nuclear receptors [14].

Testicular zinc finger protein (TZF) has a nuclear protein with a zinc finger motif [15,16]. Analysis of the open reading frame of cDNA indicates that TZF is a polypeptide of 942 amino acids residues that included three distinct domains, namely, a zinc finger domain of the Cys_2-His_2 type, four basic amino acid-rich domains (putative nuclear-localization sequences), and a myosin II-homology domain. RT-PCR analysis of expression level of mRNAs for mouse TZF shows that transcripts are highly expressed in testis and moderately in adrenal gland, prostate gland, muscle, kidney, and uterus. Fusion proteins with green fluorescence protein (GFP) also demonstrate the nuclear localization of TZF. However, the function of TZF in various organs has not been clear yet. In this paper, we describe that TZF might be a novel corepressor of AR.

Materials and methods

Plasmid constructs. Plasmid vector expressing AR-GFP fusion protein, named pAR-GFP, was constructed as described previously [17]. A plasmid construct carrying GFP-TZF fusion gene, pLP-EGFP-C1-TZF [16], was digested by *SalI* and *XhoI* to remove the vector sequence and TZF cDNA was separated to two fragments. A 2.3-kb *SalI* fragment contained an N-terminal part of TZF and a 1-kb *SalI*–*XhoI* fragment contained a C-terminus of TZF. These two fragments were inserted together into pEYFP-C1 (Clontech) vector or pFLAG-cytomegalovirus (CMV) 2 (Sigma) to produce pYFP-TZF and pFLAG-TZF-CMV. A GFP fragment of pLP-EGFP-C1-TZF was replaced with c-myc tag, to produce pLP-CMV-myc-TZF. The full length of human N-CoR in pEF1-hN-CoR-V5his6 (gifted from Dr. Jun Yanagisawa, University of Tsukuba) was inserted into *Eco*RI and *NotI* sites of pBSSK (Stratagene). *SalI* enzyme recognition site was introduced into the C-terminus of hN-CoR cDNA in pBSSK by PCR. By digesting with *Eco*RI and *SalI* restriction enzymes, hN-CoR fragment was subcloned into pFLAG-CMV2 (Sigma), resulting in pFLAG-N-CoR-CMV.

The firefly luciferase reporter plasmid, pGL3-mouse mammary tumor virus (MMTV) [17], and the expression vector for AR (pCMV-hAR) were prepared as previously described [18,19]. A 644-bp of 5′-flanking region of the prostate specific antigen (PSA) gene was amplified by KOD DNA polymerase (Toyobo, Osaka, Japan) using a set of primers: PSAP-N (5′-aggtaccgaattccacattgtttgctgc-3′) and PSAP-C (5′-tccgggtgcaggtggtaagcttgg-3′). The PCR-amplified fragment was cloned into pGL3-Basic vector (Promega, Madison, WI), resulting in pGL3-PSA.

Cell culture. COS-7 cells were purchased from Riken Cell Bank (Tokyo, Japan) and LNCaP human prostatic cancer cell line was obtained from American Type Culture Collection (Manassas, VA). Both cells were maintained in Dulbecco's modified Eagle's medium (DMEM; Sigma) with antibiotics and 10% fetal bovine serum (FBS, Cansera International, Canada). HEK293T cells were purchased from Riken Cell Bank (Tokyo, Japan) and were maintained in DMEM supplemented with antibiotics and 10% FBS (Biowest, France).

Immunostaining. COS-7 cells (2×10^4 cells/well) were cultured in the Lab-Tek II Chamber Slides (Nalge Nunc International, Naperville, IL) and transfected with pGFP-TZF using 1 μl/well of the Superfect Transfection Reagent (Qiagen GmbH, Hilden, Germany). Twenty hours after incubation, cells were washed with PBS and fixed with 50% methanol/50% acetone for 2 min at 25 °C. After the cells were blocked in 1× Block-Ace (Dainippon Pharmaceutical, Osaka, Japan), anti-SC-35 mouse monoclonal antibody (Sigma–Aldrich) was reacted with the cells in 0.1× Block-Ace for 1 h at 25 °C. Following a brief wash with TBS–Tween 20 (10 mM Tris–HCl, pH 8.0, 0.9% NaCl, and 0.05% Tween 20), horseradish peroxidase-linked anti-mouse IgG (Amersham Bioscience, Piscataway, NJ) was added in 0.1× Block-Ace as a second antibody and then the cells were incubated for 45 min at 25 °C. After being washed with TBS–Tween 20, cells were mounted in Vectorshield (Vector Laboratories, Burlingame, CA) and examined in the confocal laser scanning microscope (LSM510META, Carl Zeiss, Jena, Germany).

Laser scanning microscopy. COS-7 cells (2×10^5 cells/dish) were seeded in 35-mm glass-bottomed dishes (Asahi Techno Glass, Tokyo, Japan) and transfected with 0.5 μg/dish of a GFP-fusion construct using 5 μl of Superfect Reagent (Qiagen). In case of coexpression studies, cells were transfected with 0.5 μg/dish pAR-GFP and 2.5 μg pYFP-TZF. The cells were incubated for 20 h in DMEM supplemented with 10% of charcoal-treated FBS. Cells were observed before and after the treatment of 10^{-8} M of dihydrotestosterone (DHT) using a LSM510META invert confocal laser scanning microscope (Carl Zeiss) using a 100×, 1.4 numerical aperture oil immersion objective. Images were collected at a 12-bit depth resolution of intensities over 1024 × 1024 pixels. For excitation of GFP and YFP, 488-nm argon laser was used and each fluorescent signal was separated using the Emission Fingerprinting technique established by Carl Zeiss. A spectral signature of each emission signal was recorded as a reference spectrum and a digital unmixing was performed using the reference spectra.

Immunoprecipitation and immunoblotting. A plasmid expressing myc-tagged or GFP-fused TZF was transfected into HEK293T cells together with expression plasmid for the full-length (1–919 aa) or truncated mutants (AF-1; 1-566 aa, AF-2; 623-919 aa) of AR by using FuGENE6 reagent (Roche), and the cells were maintained with or without 10^{-8} M DHT. Whole cell extracts were prepared from lysed cells in NE buffer (20 mM Hepes–NaOH, pH 7.9, 20% glycerol, 100 mM KCl, 0.2 mM EDTA, 0.5% NP-40, and 1:100-diluted protease inhibitor cocktail). The extracts were incubated for 2 h at 4 °C with 20 μl of protein A–Sepharose (Amersham Biosciences) coupled with 10 μg of either N-20 rabbit polyclonal antibody (Santa Cruz Biotechnology) to detect the N-terminal transactivation domain fragment of AR or C-19 rabbit polyclonal antibody (Santa Cruz Biotechnology) to detect the full-length or C-terminal fragment and equilibrated with WB buffer (20 mM Hepes–NaOH, pH 7.9, 20% glycerol, 100 mM KCl, 0.2 mM EDTA, 0.5% NP-40, and 0.5% skim milk). After the matrices were washed four times with 180 μl WB buffer and four times with 180 μl WH buffer (20 mM Hepes–NaOH, pH 7.9, 20% glycerol, 100 mM KCl, 0.2 mM EDTA, and 0.5% NP-40), bound materials were eluted with 60 μl of 2× sodium dodecyl sulfate (SDS) sample buffer, resolved on 10% SDS–polyacrylamide gel electrophoresis (PAGE), and transferred onto Immobilon-P PVDF membrane (Millipore). Myc-tagged or GFP-TZF was detected with each anti-c-myc mouse monoclonal antibody (9E10; Roche) or anti-GFP mouse monoclonal antibody (GF200; Nacalai Tesque). The full-length or N-terminal transactivation domain fragment of AR was detected with antibody N-20 and the C-terminal fragment was detected with antibody C-19.

Functional promoter assay. COS-7 or LNCaP cells (1×10^5 cells/well) were seeded in 12-well plates at 24 h before transfection. A reporter plasmid, pGL3-MMTV or pGL3-PSA (0.5 μg/well), was cotransfected with 3 ng/ml pRL-CMV (Promega) as an internal control, 0.1 μg/well pCMV-hAR, and 0.5 μg or 1.0 μg of the pFLAG-TZF-CMV2 using 1.7 μl/well of Superfect Transfection Reagent (Qiagen). Three hours after transfection, 0.5 ml of DMEM containing charcoal-treated fetal bovine serum was added with or without steroid

hormones. At 24 h post-transfection, cells were rinsed with PBS and lysed in the lysis buffer of a luciferase assay kit (Promega). The luciferase activity was assayed using a Dual-Luciferase Assay System (Promega) and Lumat LB 9507 (Berthold Technologies, Bad Wildbad, Germany). Data were presented as means ± SD. One-way analysis of variance followed by Scheffe's test was used for multigroup comparisons. A value of $P < 0.05$ was considered to be statistically significant.

Results

TZF was located close to the splicing factor compartment

TZF was located in the nucleus and formed larger size but smaller number of dots [16]. Splicing factor complexes also form subnuclear dots whose pattern was similar to that of TZF. We analyzed whether TZF and SC-35, which was shown to be located in the splicing factor complex, were colocalized in the same nuclear dots. To examine an authentic localization pattern of SC-35, immunostaining was performed using anti-SC-35 antibody. SC-35 showed clear dot pattern in the nucleus and TZF was also located close to the SC-35 spots (Fig. 1). TZF was not directly involved the splicing factor complexes but might be a mediator between the splicing factor complex and another protein complex.

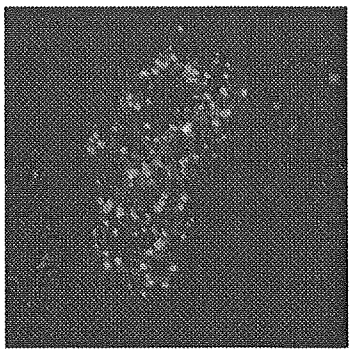

Fig. 1. Subnuclear localization of TZF and SC-35. COS-7 cells were transfected with pGFP-TZF. Twenty-four hours after transfection, cells were fixed with ethanol/acetone and treated with anti-SC-35 antibody for 1 h at 25 °C. After brief wash, second antibody was added for detection. Green signals show the localization of GFP-TZF and red signals show that of SC-35.

TZF was recruited into AR subnuclear foci after the ligand treatment

We previously showed that AR was located in the cytoplasm in the absence of the ligand. After the treatment with the ligand, AR translocated into the nucleus and formed subnuclear fine foci [17,20]. TZF was also shown to localize at the subnuclear foci [16]. To investigate the colocalization of the two proteins, pYFP-TZF and pAR-GFP were cotransfected and cells were observed using confocal laser scanning microscope. As previously reported, AR translocated from the cytoplasm to the nucleus after the treatment of DHT and subnuclear foci formation was observed (Figs. 2A and D). TZF was located in the nucleus and formed larger size but smaller number of dots without DHT compared to the AR foci (Fig. 2B). However, coexpression of AR changed the subnuclear foci pattern of TZF in the presence of the ligand (Fig. 2E). With AR and DHT, TZF formed smaller size but larger number of subnuclear dots that were similar to the AR subnuclear foci (Figs.

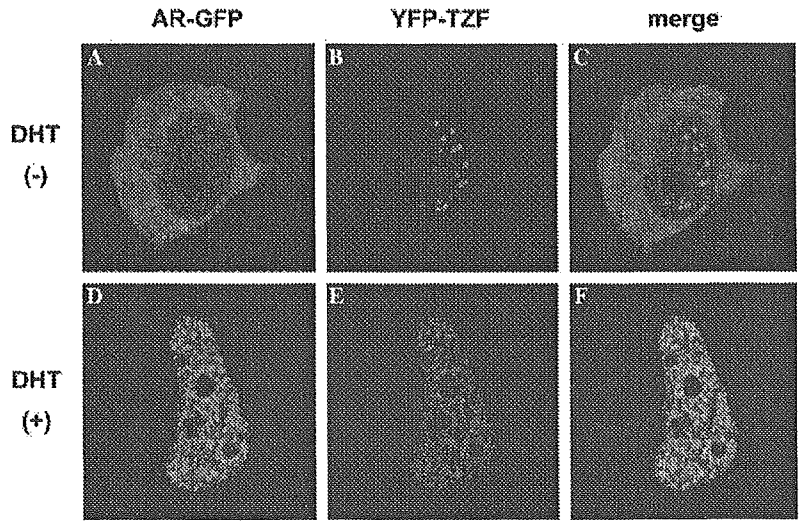

Fig. 2. Ligand-induced colocalization of AR and TZF. COS-7 cells were cotransfected with AR-GFP and YFP-TZF, and observed using the LSM510META laser scanning microscopy before and after the treatment of 10^{-8} M of DHT. Upper panels (A–C) show images before the treatment of DHT and lower panels (D–F) show images after 1 h treatment of DHT. Fluorescent signals for AR-GFP (A,D) and YFP-TZF (B,E) were obtained and two signals were merged (C,F). GFP (A, C, D, and F) and YFP (B, C, E, and F) signals are represented as green and red, respectively.

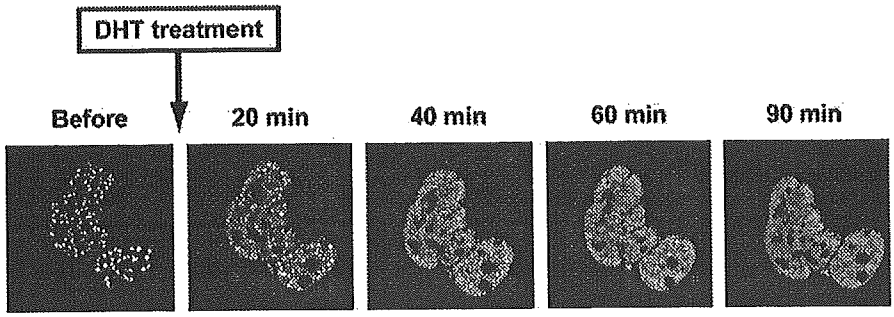

Fig. 3. Time lapse experiment for localization of TZF after the treatment of DHT. COS-7 cells transfected with pYFP-TZF and pCMV-hAR were treated with 10^{-8} M DHT. Images were collected before and 20, 40, 60, and 90 min after the DHT treatment.

2E and F). Time course experiment revealed that since 40 min after the treatment the size of TZF dots started to become smaller with the coexpression of AR (Fig. 3). These data suggested that TZF was recruited into the AR subnuclear foci in the presence of the ligand.

Protein–protein interactions between TZF and AR

Immunocoprecipitation experiments using whole cell extracts were performed to test whether or not TZF binds to AR in living cells. Each plasmid expressing GFP-fused TZF and the full length of AR was transfected into HEK293T cells, and then the cells were maintained with 10^{-8} M DHT. GFP-fused TZF was precipitated with the full-length AR in the presence of DHT (Fig. 4A). Next, a plasmid expressing myc-tagged TZF was transfected into HEK293T cells together with expression plasmid for the AR-(1–532) covering AF-1 or AR-(622–919) covering the ligand binding domain AF-2, and then the cells were maintained with or without 10^{-8} M DHT. Myc-tagged TZF was specifically precipitated with AF-1, which exists in the nucleus without DHT [20], in a ligand-independent fashion (Fig. 4B). By contrast, TZF did not bind to AF-2 in the presence of DHT (Fig. 4C).

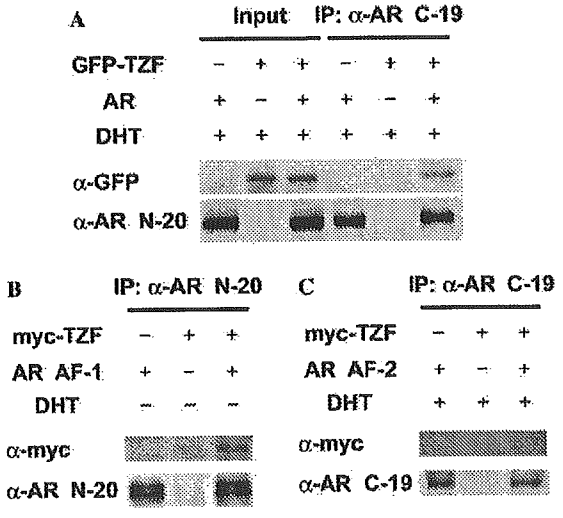

Fig. 4. TZF interacts with the full-length AR or AR-AF-1. (A) Coimmunoprecipitation of GFP-TZF with full-length AR. GFP-TZF and full-length AR were coexpressed in HEK293T cells. The cells were treated with 10^{-8} M DHT, collected at 48 h after transfection, and lysed in NE buffer. Portions of the lysates were immunoblotted with the anti-GFP or the anti-AR N-20 antibody (input), and the rest of the samples were immunoprecipitated with the anti-AR C-19 antibody followed by immunoblotting with the anti-GFP or the anti-AR N-20 antibody (IP). (B) Coimmunoprecipitation of myc-tagged TZF with AR-AF-1 (1–566 aa). (C) Coimmunoprecipitation of myc-tagged TZF with AR-AF-2 (623–919 aa).

TZF repressed AR-mediated transcriptional activation

To examine an effect of TZF on AR-mediated transcriptional activation, we performed luciferase assay using the MMTV-luciferase reporter gene in COS-7 cells. Surprisingly, expression of TZF repressed DHT-induced transcriptional activation by AR in a dose-dependent manner (Fig. 5A). We confirmed the repression by TZF using a different cell line (LNCaP; prostatic carcinoma cells, Fig. 5B) and a different promoter (PSA; prostate specific antigen, Fig. 5C).

N-CoR expression caused no significant effects on TZF-induced repression for AR-mediated transactivation

N-CoR is well known as a corepressor for nuclear receptors. N-CoR is supposed to recruit histone deacetylase into the nuclear receptor complex to repress the AR-mediated transcriptional activation [21]. To examine whether N-CoR was involved in the repression by TZF, luciferase assay was performed using cells coexpressing AR, N-CoR, and TZF. Both N-CoR and TZF repressed the AR-mediated transcriptional activation by itself (Fig. 6). Coexpression of these two proteins exhibited an additive effect in the repression. We have not obtained a clear evidence for direct relationship between TZF and N-CoR in the present study.

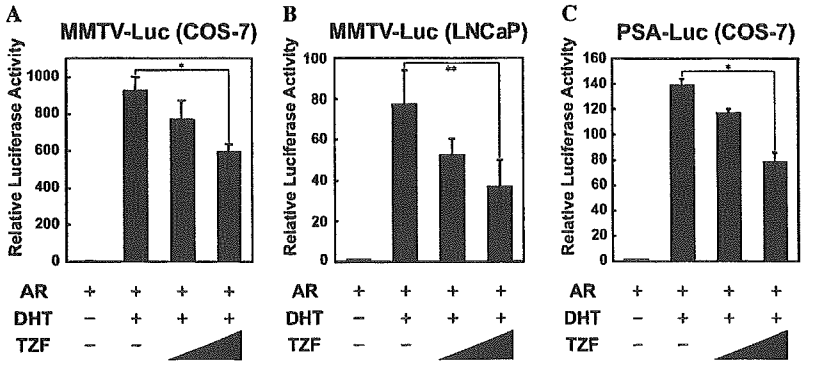

Fig. 5. Repression of AR-mediated transcriptional activation by TZF. (A,B) COS-7 (A) or LNCaP (B) cells were transiently transfected with 0.3 μg pGL3-MMTV, 3 ng pRL-CMV, 0.1 μg pCMV-hAR, and 0.5 or 1 μg pFLAG-TZF-CMV, as indicated. After 24 h incubation with or without 10^{-8} M of DHT, cells were lysed and whole cell extracts were subjected to the luciferase assay. (C) COS-7 cells were cotransfected with 0.3 μg pGL3-prostate specific antigen (PSA), 3 ng pRL-CMV, 0.1 μg pAR-CMV, and 0.5 or 1 μg pFLAG-TZF-CMV and luciferase assay was performed as above. Bars show the fold change in the luciferase activity relative to the value by the wild type AR without DHT. The average of three independent experiments is shown with the standard deviation. $*P < 0.01$; $**P < 0.05$.

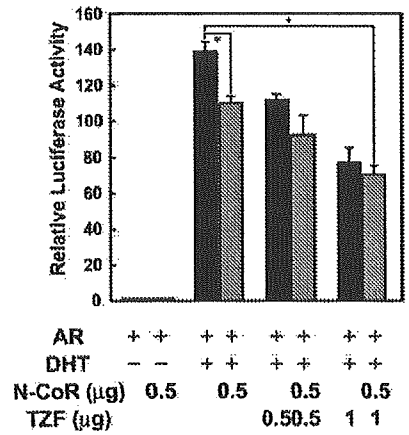

Fig. 6. The effect of N-CoR expression on the repression of AR-mediated transcriptional activation by TZF. COS-7 cells were cotransfected with 0.3 μg pGL3-PSA, 3 ng pRL-CMV, 0.1 μg pCMV-hAR, and 0.5 or 1 μg pFLAG-TZF-CMV with or without 0.5 μg pFLAG-N-CoR-CMV and treated with or without 10^{-8} M DHT. Luciferase assay was performed after 24 h incubation. Solid bars show the values without N-CoR and shadow bars show those with N-CoR. Bars show the fold change in the luciferase activity relative to the value without DHT. The mean values and the standard deviation from three independent experiments are shown. $*P < 0.01$.

Discussion

Transcriptional repression is an intrinsic part of endocrine physiology and contributes to feedback regulation associated with the inhibition of the physiologic response. To date, several investigators have found transcriptional corepressors, such as SMRT [10] and N-CoR [12]. However, there is little information on the effects and action mechanisms of corepressors. In the present study, we demonstrated that a zinc finger protein TZF formed specific foci located close to the splicing factor compartment in nuclei and was recruited into the AR foci in the present of DHT. Functional reporter assays and the immunoprecipitation experiments also showed that the TZF was essentially the AR-AF-1-interacting transcriptional corepressor.

In the nucleus, there exist different sets of functional compartments often called "foci" or "speckles," which include the splicing factor compartment (SFC) that consists of nearly 20–50 large foci [22], and nuclear receptor foci possibly associated with the nuclear matrix structures [17,23,24]. We first visualized TZF-dependent compartment in nuclei and showed that TZF-dependent foci were located close to the splicing factor compartment. Furthermore, TZF interacted to the AR-AF-1 sequence (Fig. 3). It has been known that various molecules, such as SRA [25], BRCA1 [26], and cyclin E [27], bind to the AR-AF-1 and that these molecules are involved in splicing activity of RNA molecules. Together with the finding that TZF-dependent foci were located close to SC-35 compartment, TZF may be involved in the spliceosomal machinery.

Next, we visualized the spatial relationship between TZF-dependent foci and AR foci in the presence and the absence of DHT. Interestingly, by the addition of DHT, TZF was recruited into AR foci from TZF-dependent foci in a time-dependent fashion and, after 90 min, TZF molecules were completely collocated to AR foci (Figs. 2 and 3). The formation of AR foci with the presence of ligand in nuclei plays an important role on its transcriptional activity [17,20]. Therefore, we examined whether TZF was involved in the AR-mediated transcriptional activation. Consequently, we obtained the results that TZF decreased the AR-mediated transcriptional activation. These results suggested that the binding of TZF with AR might play a key role in the transcriptional activity of AR.

AR has been thought to be quite unique among the nuclear receptor superfamily members, because most of its activities are mediated through the ligand-independent constitutive activity of AF-1 function [28]. In addition, the interaction of the N- and C-terminal domain is important for exerting the full AR transactivation capacity [29–31]. Most of the transcriptional cofactors reported are known to interact with AF-2, the number of transcriptional cofactors specifically interacting with the AF-1 sequence of AR is limited. For example, CBP/p300 [7] and SRC-1 [29] interact with both AF-1 and AF-2, and N-CoR [21] and SMRT [32] also bind to AF-2 of AR protein. We, in the present study, showed that TZF interacted with AF-1 domain of AR molecule. Therefore, TZF is a unique corepressor associating with the AR-AF-1 domain.

N-CoR and SMRT contain CoRNR motifs (L/I-X-X-V/I-I) that interact with nuclear hormone receptors. Therefore, we searched the sequence of motifs in TZF protein but were not able to find it. N-CoR is supposed to recruit histone deacetylase into the nuclear receptor complex to repress the AR-mediated transcriptional activation. To examine whether N-CoR was involved in the repression by TZF, we performed luciferase assay using cells coexpressing AR, N-CoR, and TZF. Both N-CoR and TZF repressed the AR-mediated transcriptional activation by itself (Fig. 6). Furthermore, coexpression of these two proteins exhibited an additive effect in the repression. These results show that TZF and N-CoR might act through the different pathways or mechanism on the repression of the AR-mediated transcriptional activation.

To examine an effect of TZF on the AR-mediated transcriptional activation, we performed luciferase assay using the MMTV-luciferase reporter gene in COS-7 cells. Expression of TZF repressed DHT-induced transcriptional activation by AR in a dose-dependent manner (Fig. 5A). We also confirmed the repression by TZF using prostatic carcinoma cells (Fig. 5B) and a different promoter (Fig. 5C). Thus, TZF might be a novel corepressor of AR. Recently, it has been reported that abnormalities of coactivators or corepressors caused several diseases and they were named as cofactor diseases. Rubinstein–Taybi syndrome, that exhibits facial abnormalities, broad thumbs, broad big toes, and mental retardation as the main clinical features, is caused by mutations in the transcriptional coactivator CBP [33]. Some patients with androgen insensitivity syndrome lack a coactivator interacting with the AF-1 region of the androgen receptor [19]. By contrast, repression of transcriptional activation of nuclear receptors plays important roles in acute promyelocytic leukemia and other diseases [34]. Our previous studies revealed that transcripts of TZF were expressed in testis [15]. In particulate, elevated expression of the transcript during testicular development in mice was restricted to spermatocytes at the pachytene stage of meiotic prophase, and to round and elongated spermatids. However, it is unclear now whether the decrease of the transcriptional activation of AR by TZF affects the testis. To fully elucidate the action and mechanism of TZF in the body, we have to wait for the preparation of *tzf*-deficient mouse.

Acknowledgments

This work was in part supported by Grants-in-Aid for Scientific Research from The Ministry of Education, Culture, Sports, Science and Technology of Japan and by grants from the Smoking Research Foundation.

References

[1] D.J. Mangelsdorf, R.M. Evans, The RXR heterodimers and orphan receptors, Cell 83 (1995) 841–850.
[2] A. Aranda, A. Pascual, Nuclear hormone receptors and gene expression, Physiol. Rev. 81 (2001) 1269–1304.
[3] Y. Kamei, L. Xu, T. Heinzel, J. Torchia, R. Kurokawa, B. Gloss, S.C. Lin, R.A. Heyman, D.W. Rose, C.K. Glass, M.G. Rosenfeld, A CBP integrator complex mediates transcriptional activation and AP-1 inhibition by nuclear receptors, Cell 85 (1996) 403–414.
[4] C.A. Heinlein, C. Chang, Androgen receptor (AR) coregulators: an overview, Endocr. Rev. 23 (2002) 175–200.
[5] T. Heinzel, R.M. Lavinsky, T.M. Mullen, M. Soderstrom, C.D. Laherty, J. Torchia, W.M. Yang, G. Brard, S.D. Ngo, J.R. Davie, E. Seto, R.N. Eisenman, D.W. Rose, C.K. Glass, M.G. Rosenfeld, A complex containing N-CoR, mSin3 and histone deacetylase mediates transcriptional repression, Nature 387 (1997) 43–48.
[6] E. Kalkhoven, J.E. Valentine, D.M. Heery, M.G. Parker, Isoforms of steroid receptor co-activator 1 differ in their ability to potentiate transcription by the oestrogen receptor, EMBO J. 17 (1998) 232–243.
[7] V.V. Ogryzko, R.L. Schiltz, V. Russanova, B.H. Howard, Y. Nakatani, The transcriptional coactivators p300 and CBP are histone acetyltransferases, Cell 87 (1996) 953–959.
[8] V.V. Ogryzko, T. Kotani, X. Zhang, R.L. Schiltz, T. Howard, X.J. Yang, B.H. Howard, J. Qin, Y. Nakatani, Histone-like TAFs within the PCAF histone acetylase complex, Cell 94 (1998) 35–44.
[9] M. Ito, C.X. Yuan, S. Malik, W. Gu, J.D. Fondell, S. Yamamura, Z.Y. Fu, X. Zhang, J. Qin, R.G. Roeder, Identity between TRAP and SMCC complexes indicates novel pathways for the function of nuclear receptors and diverse mammalian activators, Mol. Cell 3 (1999) 361–370.
[10] J.D. Chen, R.M. Evans, A transcriptional co-repressor that interacts with nuclear hormone receptors, Nature 377 (1995) 454–457.
[11] A.J. Horlein, A.M. Naar, T. Heinzel, J. Torchia, B. Gloss, R. Kurokawa, A. Ryan, Y. Kamei, M. Soderstrom, C.K. Glass, M.G. Rosenfeld, Ligand-independent repression by the thyroid hormone receptor mediated by a nuclear receptor co-repressor, Nature 377 (1995) 397–404.
[12] J.D. Chen, K. Umesono, R.M. Evans, SMRT isoforms mediate repression and anti-repression of nuclear receptor heterodimers, Proc. Natl. Acad. Sci. USA 93 (1996) 7567–7571.

[13] S. Sande, M. Privalsky, Identification of TRACs (T3 receptor-associating cofactors), a family of cofactors that associate with, and modulate the activity of, nuclear hormone receptors, Mol. Endocrinol. 10 (1996) 813–825.
[14] M. Beato, S. Chavez, M. Truss, Transcriptional regulation by steroid hormones, Steroids 61 (1996) 240–251.
[15] A. Inoue, A. Ishiji, S. Kasagi, M. Ishizuka, S. Hirose, T. Baba, H. Hagiwara, The transcript for a novel protein with a zinc finger motif is expressed at specific stages of mouse spermatogenesis, Biochem. Biophys. Res. Commun. 273 (2000) 398–403.
[16] M. Ishizuka, H. Ohshima, N. Tamura, T. Nakada, A. Inoue, S. Hirose, H. Hagiwara, Molecular cloning and characteristics of a novel zinc finger protein and its splice variant whose transcripts are expressed during spermatogenesis, Biochem. Biophys. Res. Commun. 301 (2003) 1079–1085.
[17] A. Tomura, K. Goto, H. Morinaga, M. Nomura, T. Okabe, T. Yanase, R. Takayanagi, H. Nawata, The subnuclear three-dimensional image analysis of androgen receptor fused to green fluorescence protein, J. Biol. Chem. 276 (2001) 28395–28401.
[18] R. Nakao, M. Haji, T. Yanase, A. Ogo, R. Takayanagi, T. Katsube, Y. Fukumaki, H. Nawata, A single amino acid substitution (Met786–Val) in the steroid-binding domain of human androgen receptor leads to complete androgen insensitivity syndrome, J. Clin. Endocrinol. Metab. 74 (1992) 1152–1157.
[19] M. Adachi, R. Takayanagi, A. Tomura, K. Imasaki, S. Kato, K. Goto, T. Yanase, S. Ikuyama, H. Nawata, Androgen-insensitivity syndrome as a possible coactivator disease, N. Engl. J. Med. 343 (2000) 856–862.
[20] M. Saitoh, R. Takayanagi, K. Goto, A. Fukamizu, A. Tomura, T. Yanase, H. Nawata, The presence of both the amino- and carboxyl-terminal domains in the AR is essential for the completion of a transcriptionally active form with coactivators and intranuclear compartmentalization common to the steroid hormone receptors: a three-dimensional imaging study, Mol. Endocrinol. 16 (2002) 694–706.
[21] S. Cheng, S. Brzostek, S.R. Lee, A.N. Hollenberg, S.P. Balk, Inhibition of the dihydrotestosterone-activated androgen receptor by nuclear receptor corepressor, Mol. Endocrinol. 16 (2002) 1492–1501.
[22] T. Misteli, Cell biology of transcription and pre-mRNA splicing: nuclear architecture meets nuclear function, J. Cell. Sci. 113 (2000) 1841–1849.
[23] H. Htun, J. Barsony, I. Renyi, D.L. Gould, G.L. Hager, Visualization of glucocorticoid receptor translocation and intranuclear organization in living cells with a green fluorescent protein chimera, Proc. Natl. Acad. Sci. USA 93 (1996) 4845–4850.
[24] G. Fejes-Toth, D. Pearce, A. Naray-Fejes-Toth, Subcellular localization of mineralocorticoid receptors in living cells: effects of receptor agonists and antagonists, Proc. Natl. Acad. Sci. USA 95 (1998) 2973–2978.
[25] R.B. Lanz, N.J. McKenna, S.A. Onate, U. Albrecht, J. Wong, S.Y. Tsai, M.J. Tsai, B.W. O'Malley, A steroid receptor coactivator, SRA, functions as an RNA and is present in an SRC-1complex, Cell 97 (1999) 17–27.
[26] J.J. Park, R.A. Irvine, G. Buchanan, S.S. Koh, J.M. Park, W.D. Tilley, M.R. Stallcup, M.F. Press, G.A. Coetzee, Breast cancer susceptibility gene 1 (BRCAI) is a coactivator of the androgen receptor, Cancer Res. 60 (2000) 5946–5949.
[27] A. Yamamoto, Y. Hashimoto, K. Kohri, E. Ogata, S. Kato, K. Ikeda, M. Nakanishi, Cyclin E as a coactivator of the androgen receptor, J. Cell. Biol. 150 (2000) 873–880.
[28] B. He, J.A. Kemppainen, J.J. Voegel, H. Gronemeyer, E.M. Wilson, Activation function 2 in the human androgen receptor ligand binding domain mediates interdomain communication with the NH(2)-terminal domain, J. Biol. Chem 274 (1999) 37219–37225.
[29] C.L. Bevan, S. Hoare, F. Claessens, D.M. Heery, M.G. Parker, The AF1 and AF2 domains of the androgen receptor interact with distinct regions of SRC1, Mol. Cell. Biol. 19 (1999) 8383–8392.
[30] P. Doesburg, C.W. Kuil, C.A. Berrevoets, K. Steketee, P.W. Faber, E. Mulder, A.O. Brinkmann, J. Trapman, Functional in vivo interaction between the amino-terminal, transactivation domain and the ligand binding domain of the androgen receptor, Biochemistry 36 (1997) 1052–1064.
[31] C.A. Berrevoets, P. Doesburg, K. Steketee, J. Trapman, A.O. Brinkmann, Functional interactions of the AF-2 activation domain core region of the human androgen receptor with the amino-terminal domain and with the transcriptional coactivator TIF2 (transcriptional intermediary factor2), Mol. Endocrinol. 12 (1998) 1172–1183.
[32] G. Liao, L.Y. Chen, A. Zhang, A. Godavarthy, F. Xia, J.C. Ghosh, H. Li, J.D. Chen, Regulation of androgen receptor activity by the nuclear receptor corepressor SMRT, J. Biol. Chem. 278 (2003) 5052–5061.
[33] F. Petrij, R.H. Giles, H.G. Dauwerse, J.J. Saris, R.C.M. Hennekam, M. Masuno, N. Tommerup, G.J.B. van Ommen, R.H. Goodman, D.J.M. Peters, M.H. Breuning, Rubinstein–Taybi syndrome caused by mutations in the transcriptional co-activator CBP, Nature 376 (1995) 348–351.
[34] X. Hu, M.A. Lazar, Transcriptional repression by nuclear hormone receptors, Trends Endocrinol. Metab. 11 (2000) 6–10.

Available online at www.sciencedirect.com
SCIENCE DIRECT®
Toxicology and Applied Pharmacology 207 (2005) 187–194
Toxicology and Applied Pharmacology
www.elsevier.com/locate/ytaap

Excess L-arginine restores endothelium-dependent relaxation impaired by monocrotaline pyrrole

Wei Cheng[a,1], Masahiro Oike[a,*], Masakazu Hirakawa[a], Keizo Ohnaka[b], Tetsuya Koyama[a], Yushi Ito[a]

[a]*Department of Pharmacology, Graduate School of Medical Sciences, Kyushu University, Fukuoka 812-82, Japan*
[b]*Department of Geriatric Medicine, Graduate School of Medical Sciences, Kyushu University, Fukuoka 812-82, Japan*

Received 9 November 2004; accepted 5 January 2005
Available online 25 February 2005

Abstract

The pyrrolizidine alkaloid plant toxin monocrotaline pyrrole (MCTP) causes pulmonary hypertension in experimental animals. The present study aimed to examine the effects of MCTP on the endothelium-dependent relaxation. We constructed an in vitro disease model of pulmonary hypertension by overlaying MCTP-treated bovine pulmonary artery endothelial cells (CPAEs) onto pulmonary artery smooth muscle cell-embedded collagen gel lattice. Acetylcholine (Ach) induced a relaxation of the control CPAEs-overlaid gels that were pre-contracted with noradrenaline, and the relaxation was inhibited by L-NAME, an inhibitor of NO synthase (NOS). In contrast, when MCTP-treated CPAEs were overlaid, the pre-contracted gels did not show a relaxation in response to Ach in the presence of 0.5 mM L-arginine. Expression of endothelial NOS protein, Ach-induced Ca^{2+} transients and cellular uptake of L-[^{3}H]arginine were significantly smaller in MCTP-treated CPAEs than in control cells, indicating that these changes were responsible for the impaired NO production in MCTP-treated CPAEs. Since cellular uptake of L-[^{3}H]arginine linearly increased according to its extracellular concentration, we hypothesized that the excess concentration of extracellular L-arginine might restore NO production in MCTP-treated CPAEs. As expected, in the presence of 10 mM L-arginine, Ach showed a relaxation of the MCTP-treated CPAEs-overlaid gels. These results indicate that the impaired NO production in damaged endothelial cells can be reversed by supplying excess L-arginine.

Keywords: Monocrotaline; Nitric oxide; L-arginine; Endothelium; Pulmonary hypertension

Introduction

Experimental animal model of pulmonary hypertension (PH) has been created either by exposing animals to hypoxia or a metabolite of the pyrrolizidine alkaloid plant toxin monocrotaline. Hypoxia is known to induce the spasm of pulmonary artery thereby inducing PH. In contrast, cause of PH induced by monocrotaline, especially its toxic metabolite monocrotaline pyrrole (MCTP), is still controversial.

It is well known that MCTP induces megalocytic change in pulmonary artery endothelial cells, which would induce the prolonged activation of vascular remodeling and cause PH (Reindel and Roth, 1991). It was reported that the MCTP-induced inhibition of cdc2 kinase may lead to prolonged cell cycle arrest and subsequent megalocytic change in endothelium (Thomas et al., 1998). Recent reports suggest another possibility that the MCTP-induced megalocytic change may be due to the blockade of Golgi trafficking, thereby leading to the disruption of caveolin-1α (cav-1α)/raft function and mitosis sensor function of Golgi (Mathew et al., 2004; Shah et al., in press). Furthermore, Ito et al. (2000) examined the functional alteration of MCTP-treated vessels and showed the elevation of the resting membrane potential and the impaired endothelium-derived relaxation in pulmonary arteries of

* Corresponding author. Fax: +81 92 642 6079.
E-mail address: moike@pharmaco.med.kyushu-u.ac.jp (M. Oike).
[1] Present address: Department of Pharmacology, Jinzhou Medical College, Jinzhou 121001, China.

0041-008X/$ - see front matter © 2005 Elsevier Inc. All rights reserved.
doi:10.1016/j.taap.2005.01.002

MCTP-treated rats. It was also reported that the expression level of endothelial NOS (eNOS) protein was altered in PH model rats (Tyler et al., 1999). Another group reported that the expression of eNOS mRNA and protein were not altered in the lungs of MCTP-treated rats but the increased oxidative stress resulted in the low bioavailability of NO (Mathew et al., 2002). Therefore, it can be considered that the elevation of local NO concentration would be a promising approach for the treatment of PH.

Inhalation of NO gas is known to induce pulmonary vasodilation, thereby being regarded as a feasible remedy for cardiovascular diseases including PH (Gianetti et al., 2002; Rubin, 1997). However, technical difficulties of NO inhalation and the short half life of the gas have limited its use mainly to hospitalized patients. Therefore, another approach would be to increase endogenous endothelial NO productivity and/or its action. Sildenafil, an inhibitor of cGMP phosphodiesterase, was reported to reduce pulmonary pressure in PH (Wilkens et al., 2001). Gene transfer of eNOS has also shown to reduce pulmonary artery pressure in animal model of PH of eNOS-deficient mice (Champion et al., 2002) and MCTP-treated rats (Campbell et al., 1999).

In the present study, we have focused on endothelial function, especially the productivity of NO, in calf pulmonary artery endothelial cells (CPAEs) that were treated with MCTP. Endothelial NO production is mainly obtained by the elevation of intracellular Ca^{2+} concentration ($[Ca^{2+}]_i$) that activates eNOS (Moncada et al., 1991). Therefore, we examined the effects of MCTP on NO production, $[Ca^{2+}]_i$ and the expression of eNOS in CPAEs. We have also introduced a novel method to examine endothelium-derived vasorelaxation by using an in vitro model vessel (Kimura et al., 2004) to investigate NO productivity in MCTP-treated CPAEs. Obtained results demonstrate that NO productivity can be restored by increasing the substrate of eNOS, L-arginine, even in damaged endothelial cells.

Methods

Cell culture. CPAEs were purchased from American Type Culture Collection (Manassas, VA) and cultured in Dulbecco's Modified Eagle Medium (DMEM) supplemented with 20% fetal bovine serum (FBS). Pulmonary arteries from 1-year calves were obtained from a local slaughterhouse, smooth muscle cells (BPSMCs) were cultured in DMEM with 10% FBS by explant method (Chamley et al., 1977). All cells were stored at −80 °C before use.

Assessment of cell number and cell size. For assessing the effects of MCTP on the number and the size of CPAEs, cells were seeded on 35 mm culture dish at a density of 5000 cells/cm^2, and cultured in the absence or presence of MCTP. Cells were collected by trypsinization, and the cell numbers were manually counted with a hemocytometer.

Cell size of CPAEs was measured with an image analysis software (Photoshop, Adobe Systems Inc., San Jose, CA) from the microscopic images taken with a CCD camera mounted on a microscope (Diaphot TMD; Nikon, Tokyo, Japan).

In vitro model vessel system. Gel contraction assay was performed to examine the production of vasoactive agents in CPAEs. MCTP-treated CPAEs were obtained with trypsinization after being cultured in the presence of 1 μg/ml MCTP for 5 days, and stored at −80 °C before use. BPSMCs were embedded in collagen gel at a density of 4×10^5 cells/ml in 24-well culture plate as previously reported (Kimura et al., 2002). After being cultured for 24 h, control or MCTP-treated CPAEs were overlaid onto the collagen gel at a density of 2×10^4 cells/cm^2, and allowed to spread on the gel surface for further 24 h (see cartoons in Fig. 2).

The culture plate was placed on a hot plate (MP-10DM; Kitazato Supply, Shizuoka, Japan) and kept at 37 °C throughout the measurement. The gel images were captured with a digital camera (QV-800SX, Casio, Tokyo, Japan) every 1 min. Gel contraction was then evaluated by measuring its surface area with an image analysis software (Photoshop, Adobe Systems Inc.). Measured values were normalized to the control gel area that was obtained before the application of noradrenaline.

Measurement of intracellular Ca^{2+} concentration. Intracellular Ca^{2+} concentration ($[Ca^{2+}]_i$) was measured with fura-2 fluorescence. CPAEs were loaded with fura-2/AM (Dojindo, Kumamoto, Japan) and excited at two alternative wavelengths (340 nm and 380 nm) at a rate of approximately 1 Hz. Fluorescent ratio (R) calculated from fluorescence intensities of 510 nm wavelength was converted into apparent Ca^{2+} concentration with an equation,

$$[Ca^{2+}]_i = K_{eff}\ (R - R_{min})/(R_{max} - R),$$

where K_{eff} is the "effective binding constant", R_{min} the fluorescent ratio at zero calcium and R_{max} that at high Ca^{2+}.

ECL Western blotting. Expression of eNOS protein in control and MCTP-treated CPAEs were assessed by chemiluminescence (ECL) Western blotting (ECL phosphorylation detection system, Amersham Pharmacia Biotech, Uppsala, Sweden). A constant amount of cellular protein (50 μg protein per lane) was separated with SDS-PAGE, and eNOS was detected with anti-eNOS polyclonal antibody (StressGen Biotechnologies, Co., San Diego, CA). Expression of β-actin protein was also assessed as an internal control, using monoclonal anti-β-actin antibody (Sigma). Emitted chemiluminescence was detected and analyzed with a lumino image analyzer (FAS-1000, Toyobo, Osaka, Japan).

Measurement of cellular L-[^{3}H]arginine uptake. For the measurement of cellular uptake of L-[^{3}H]arginine (Amershan, Uppsala, Sweden), control and MCTP-treated CPAEs

were seeded on 6-well culture plates at densities of 15,000 and 30,000 cells per well, respectively. To determine the concentration dependence of cellular L-[^{3}H]arginine uptake in MCTP-treated CPAEs, 1 ml of Hanks' balanced salt solution (HBSS) either with 0.3, 1 or 3 μCi/ml L-[^{3}H]arginine was placed on each well. Total uptake of L-[^{3}H]arginine in control CPAEs was determined by placing 1 ml of HBSS with 1 μCi/ml L-[^{3}H]arginine. Other details are descried previously (Kimura et al., 2004).

Drugs and solutions. Modified Krebs solution (1.5 mM Ca^{2+} solution) was used as the standard extracellular solution, containing (in mM): 132 NaCl, 5.9 KCl, 1.2 $MgCl_2$, 1.5 $CaCl_2$, 11.5 glucose, 11.5 HEPES; pH was adjusted to 7.3 with NaOH.

MCTP was prepared from crotaline (Sigma, St. Louis, MO) and o-chloranil (Sigma) with the method described by Mattocks et al. (1989), which would yield practically pure MCTP. It should be noted that the concentration of MCTP used in the present study was that of the refined product. All other drugs used in the present experiment were also obtained form Sigma (St. Louis, MO).

Statistics. Pooled data are given as mean ± SEM, and statistical significance was determined using Student's unpaired *t* test. Probabilities less than 5% ($P < 0.05$) were regarded as significant.

Results

Effects of monocrotaline pyrrole (MCTP) on cell number and cell surface area of CPAEs

Firstly, we examined the effects of MCTP on cell area and cell number in CPAEs. Single application of more than 1 μg/ml of MCTP induced the enlargement of CPAEs (Figs. 1A and Ba) and the reduction in cell number (Fig. 1Bb). MCTP-induced enlargement of CPAEs was irreversible, and persisted even after removing MCTP from culture medium or after subculture. In the following experiments, therefore, we harvested the cells after incubating with 1 μg/ml MCTP for 5 days, and stored at −80 °C until use.

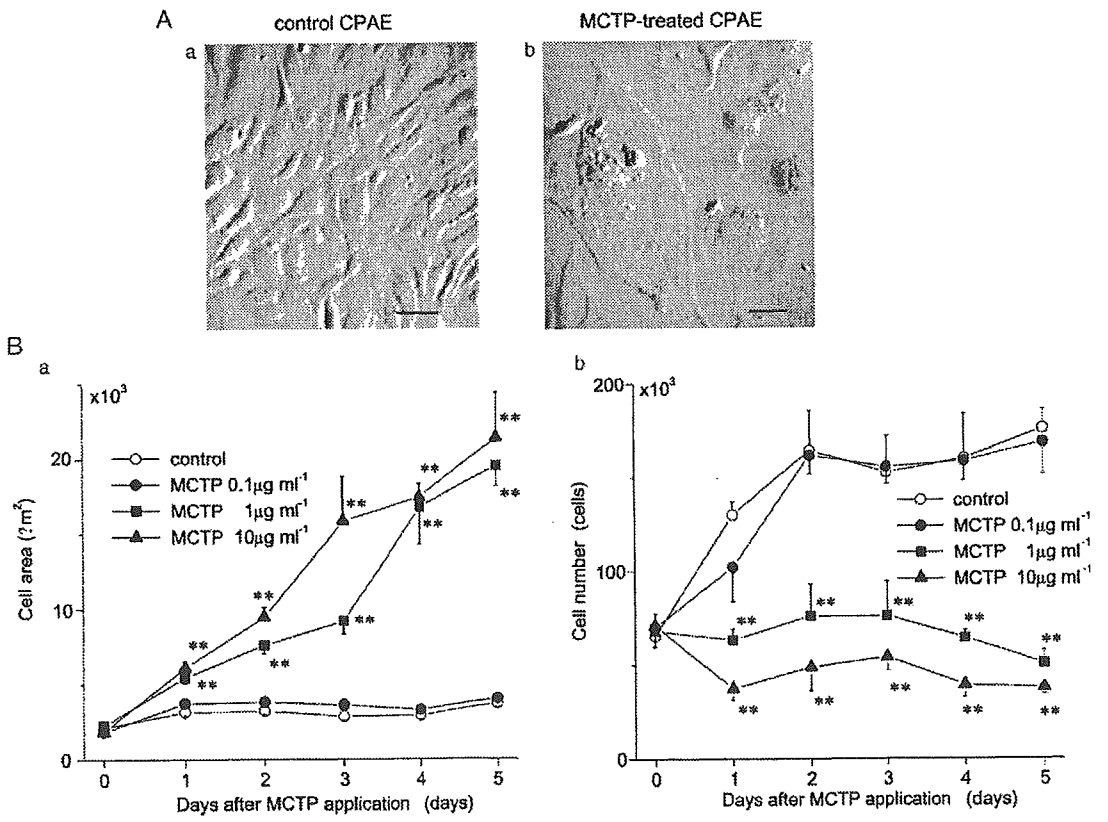

Fig. 1. Effects of monocrotaline pyrrole (MCTP) on cell surface area and cellular proliferation in calf pulmonary artery endothelial cells (CPAEs). (A) Microscopic images of control (a) and MCTP (1 μg/ml)-treated (b) CPAEs. In panel b, CPAEs were incubated with MCTP for 5 days. Each scale bar indicates 50 μm. (B) Time-dependent changes of cell area (a) and cell number (b) in CPAEs. Cells were seeded on 35 mm culture dish at a density of 5000 cells/cm^2, and cultured in the absence and presence of MCTP. $^{**}P < 0.01$ vs. untreated control.

In vitro model vessel using MCTP-treated CPAEs

We have previously reported that cultured vascular smooth muscle cells restore contractility by being embedded in three dimensional collagen gel lattice (Kimura et al., 2002, 2004). Furthermore, we have shown that endothelium-overlaid, smooth muscle cells-embedded gels show relaxation in response to Ach due to the generation of NO (Kimura et al., 2004). Therefore, we then examined the functions of the MCTP-treated CPAEs by using this in vitro model vessel system (see cartoons in Fig. 2).

BTSMCs-embedded collagen gels showed contraction in response to 1 μM noradrenaline. Subsequent application of 1 μM Ach induced a relaxation of the gel when control endothelium was overlaid (Fig. 2A, open circles). Ach-induced relaxation of the gel was not observed in the gels without overlaying CPAEs (not shown), and was significantly inhibited by L-NAME (300 μM, Fig. 2A closed circles), thereby indicating that the relaxation was due to NO production in the overlaid CPAEs. Since this measurement was performed in normal Krebs solution that does not contain L-arginine, it seems that L-arginine was supplied from DMEM in the gel. In contrast, when the same number of MCTP-treated CPAEs was overlaid on the gel, only a trace level of Ach-induced relaxation was observed (Fig. 2B), thereby suggesting that the MCTP suppressed NO productivity in CPAEs.

Ca^{2+} mobilization in MCTP-treated endothelial cells

In order to elucidate the cellular mechanisms for the impairment of NO production in MCTP-treated CPAEs, we then examined the Ach-induced $[Ca^{2+}]_i$ elevation in control and MCTP-treated CPAEs. Ach (1 μM) induced a gradual

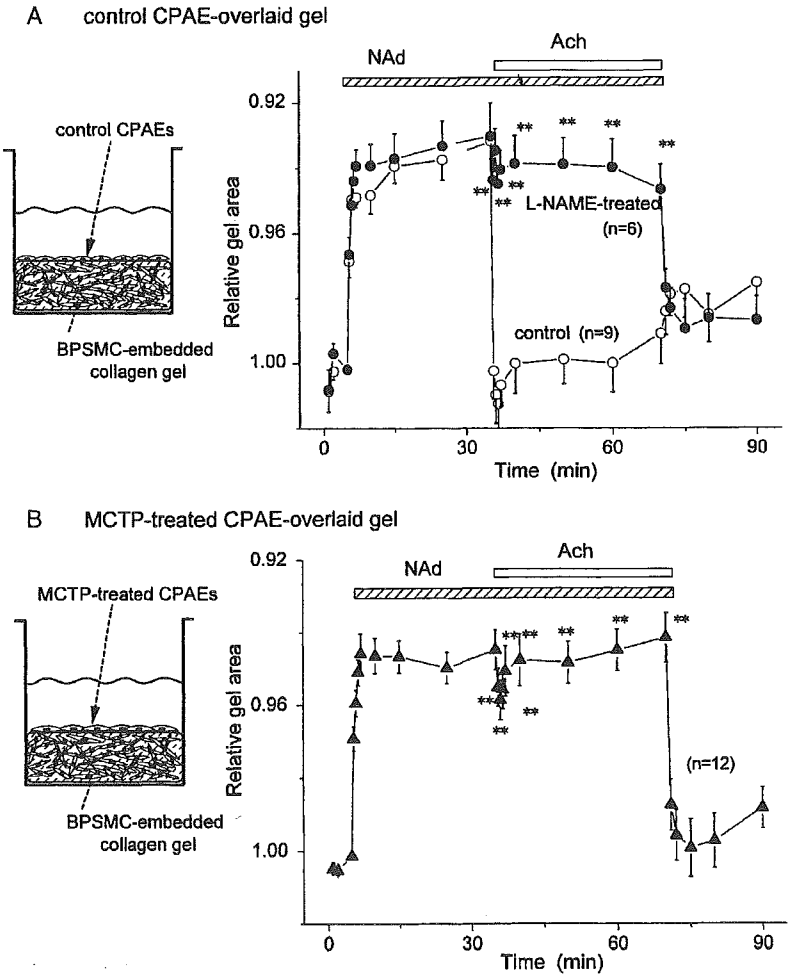

Fig. 2. In vitro model vessel assay of endothelium-dependent relaxation. Bovine pulmonary artery smooth muscle cells (BPSMCs) were embedded in collagen gel lattice, and control or MCTP-treated CPAEs were overlaid (see cartoons). (A) Control CPAEs-overlaid gels showed relaxation in response to 1 μm Ach (open circles). Pretreatment with L-NAME (0.3 mM) inhibited the relaxation (closed circles). $^{**}P < 0.01$ vs. control. (B) When MCTP-treated CPAEs were overlaid, Ach failed to induce a relaxation of the pre-contracted gels. $^{**}P < 0.01$ vs. control in A.